中介層對 CoPtCr-SiO_2 垂直式記錄媒體的影響

Effects of Intermediate Layers on CoPtCr-SiO_2 Perpendicular Recording Media

國立清華大學
材料科學工程研究所
碩士論文

指導教授：賴志煌 教授（Prof. Chih-Huang Lai)

研究生：9531574 廖容蔚（Jung-Wei Liao)

中華民國 九十七年八月

Abstract

The Hard Disk Drives (HDDs) have become the basic requirement in our life, and it is necessary to further increase the data storage capacity of the HDDs. However, the traditional longitudinal recording media meets its physical limits. So investigating a new type recording media is imperative.

In this study, CoPtCr-SiO_2 perpendicular recording media is investigated. A proper intermediate layer is needed to promote the Co hcp(00.2) texture. So at first the intermediate layers, Ta/Ru, are studied. We measured the texture of the intermediate layers by using XRD instruments. Then we investigated the effect of the dual-Ru intermediate layers that is widely used today. Besides measuring the textures of the film by using XRD instruments, we apply Vibrating Sample Magnetometer (VSM) to investigate the magnetic properties of CoPtCr-SiO_2 recording layer and some conclusions are made by the experiment results. Finally, a new material, MnRu, is proposed to be one of the possible alternative materials of the intermediate layer. The properties of the PMR film with MnRu intermediate layer are investigated.

論文摘要

在我們的生活中，硬碟已經成為一項不可或缺的生活必需品之一，且人們對硬碟容量的需求越來越大，提升硬碟的記錄密度已勢在必行。傳統的水平記錄媒體在提升記錄密度時遇到了所謂”超順磁”的極限，我們必須開發新的記錄媒體以提升記錄密度。

本研究著重於 $CoPtCr-SiO_2$ 為記錄層的垂直記錄媒體。此垂直記錄媒體的記錄層需要適當的中介層來提升其記錄層的六方晶結構，所以我們一開始先探討以 Ta 和 Ru 為主的膜層結構；我們利用 X-光繞射儀(XRD)來分析晶體結構。接著我們探討現今被廣泛使用的 Dual-Ru 膜層結構，利用震動樣品測磁力計(VSM)來量測其磁性質的表現。最後，我們提出一個代替 Ru 的材料：MnRu，利用上述的儀器來量測其結構和磁性上的表現。

致謝

在碩士班兩年的研究日子裡，可說是待在清華內最辛苦的兩年，回想起來這段期間內真的受到許多人的幫助；首先感謝賴老師的莘莘教誨，提供他在研究上寶貴的經驗給我，讓我在研究的路程上獲益非淺；而平常不斷的後面推我一把，讓我知道要不斷的努力才可以，而賴老師自己更是以身作則，帶領著我們往前衝，當我們在研究旅途上的那盞明燈。

另外感謝尖端儲存薄膜實驗室的大家，當我實驗上遇到困難的時候不嫌厭煩的指導我，在我覺得厭煩的時候開導我，因為有了大家的陪伴，使我在研究的路程上覺得並不孤單，知道有許多人跟我一起正在努力著，正在被失敗的挫折感折磨著。一個人孤單的努力和有大家一起奮鬥的感覺是絕對不一樣的，有了賴老師和大家的幫忙，我想我才能走到今天這一步。再一次的感謝大家。

最後，我想感謝我的家人總是在後面默默的支持我，不管多辛苦還是鼓勵我念書，謝謝你們。

Contents

List of Figures

List of Tables

Chapter 1 Introduction

The hard disk drives (HDDs) have been used over 50 years. The HDDs have almost become one of the basic requirements in our life today. As the prosperous growth of the internet and media, the urge to increase HDDs capacity is the current issue. To increase the HDDs capacity, decreasing the grain size of the recording layer to increase the area density is necessary. Until now, the HDDs stored information through longitudinal recording technology. When the grain size is too small that the crystalline anisotropy energy of the grain cannot overcome the thermal fluctuation, the magnetic moment in each grain is no longer stable and the effect so called "superparamagnetic effect" happens. In longitudinal recording, the superparamagnetic effect is the main limit for increasing the data stored capacity. Recently, the perpendicular magnetic recording paradigm was proposed to defer the superparamagnetic limit. In the perpendicular recording, the direction of the magnetization used as storing information is perpendicular to the film plane. When increase the areal density, the film thickness is the same, so the superparamagnetic effect can be deferred in the perpendicular recording technology. In Co-based perpendicular recording media, proper intermediate layers are needed to provide a good epitaxial condition if we want the magnetization of Co perpendicular to the plane. The basic requirements of the intermediate layer are similar lattice constants to the lattice of Co, good wettability for Co, and proper surface roughness of the intermediate layer. Until now, Ru is the most suitable material for the intermediate layer in CoPtCr-SiO_2 perpendicular recording media.

Motivation

One important issue for the current perpendicular recording media (PMR) is to decreasing the thickness of the intermediate layer. There are two main reasons. First, the writing process in the perpendicular recording is shown in Figure 1- 1. The writing field is generated from the writing head, goes through the soft underlayer (SUL) and finally comes to the tail of the writing head to form a closure loop. Decreasing the distance between the writing head and the SUL can greatly increase the effective writing field, and it can be done by reducing the thickness of the intermediate layer. Second, due to the high cost of Ru that is the most suitable material for the intermediate layer in CoPtCr-SiO_2 perpendicular recording media now, reduce the use of Ru can reduce the cost of PMR film effectively. So decreasing the thickness of Ru intermediate or to find an alternative material for Ru are important issues today.

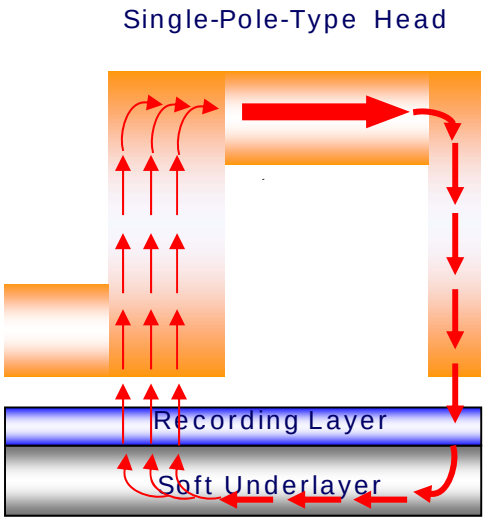

Figure 1- 1 The writing process of the PMR film

In order to go deep into this topic, we first deposited CoPtCr-SiO_2 on

Ru intermediate layer with different layer thickness or on an alternative intermediate layer by using ultra-high deposition system (UHV) in the cleanroom, measured the magnetic properties of the recording films by VSM and MOKE, and investigated the texture and the microstructure of the film by XRD and TEM. Finally, we deposited the film on the soft underlayer to be the full-stack PMR film and measure the SNR by read and write test.

Outline of the Thesis

The main part of this thesis is to discuss the effect of the intermediates on CoPtCr-SiO_2 perpendicular media. The background of the thesis is shown in Chapter 2, and previous reports of different intermediate layers are also included in Chapter 2. Chapter 3 presents the experimental and analysis techniques. In Chapter 4, the experiment results and the discussions are shown. Chapter 5 gives a brief summary of the thesis.

Chapter 2 Background

This chapter introduces the background of PMR which is discussed in this thesis. Section 2.1 presents the principles of perpendicular recording. Section 2.2 describes the different layers in the PMR and their functions. Section 2.3 is a summary of previous studies of the performance of the PMR with different underlayers. Section 2.4 gives a brief introduction of the factors that will influence the performance of the PMR.

2.1 Principles of Perpendicular Recording

2.1.1 Introduction

Hard disk drives (HDDs) have been used since the 1950s when IBM introduced random access method of accounting and control (RAMAC). Until now, the HDDs used longitudinal recording to store information. However, longitudinal recording stayed competitive for these years and delayed its rival technology. The thermal stability issue of longitudinal recording media is the physical limit that enhanced the current interest in perpendicular recording. The research on perpendicular recording media has been intense in the past five years and has received the attention of industry researchers worldwide. It is widely believed that perpendicular recording will enable us to sustain the current great strides in technological advances for the next several generations of magnetic data storage solutions.

2.1.2 Basic Concepts of Perpendicular Recording

Demagnetization fields are experienced in any ferromagnetic system and are expressed as:

$H_d=-N_dM$,

where N_d is the demagnetization factor and M is the magnetization vector. Figure 2- 1 illustrates the relation between the magnetization and the demagnetization field.

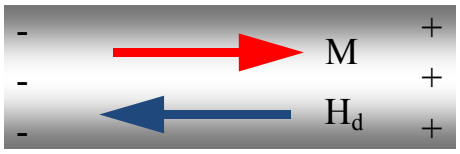

Figure 2- 1 Illustration of the magnetization and the demagnetization field

Usually, the demagnetization field is stronger when the magnetic charges are nearer.

In 1975, Iwasaki and Takemura experimentally observed that circular magnetization would be formed in a longitudinal recording technology because of demagnetizing field if thicker film were used [1]. They proposed the modern ideas of the perpendicular recording media that the magnetizations are perpendicular to the film but not parallel to the film. Figure 2- 2 shows the longitudinal media and the perpendicular media:

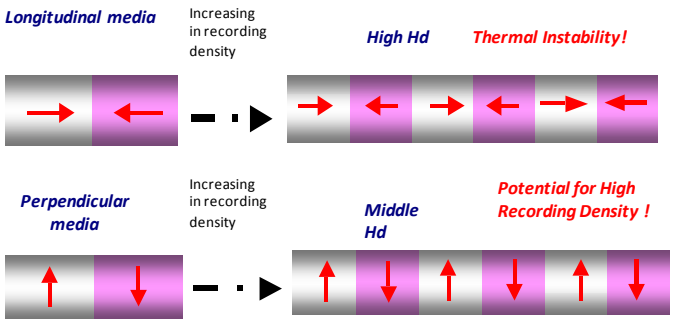

Figure 2- 2 Illustrations of the longitudinal media and the perpendicular media

In longitudinal recording, as the linearly density increases, the distance between the magnetic poles decreases. This leads to an increased demagnetization field. In perpendicular recording, the demagnetization field would be reduced at high linear densities. Therefore, perpendicular recording is a superior technique to achieve high linear density.

2.1.3 Typical Writing Process of PMR

Figure 2- 3 shows the different writing processes in longitudinal recording and perpendicular recording.

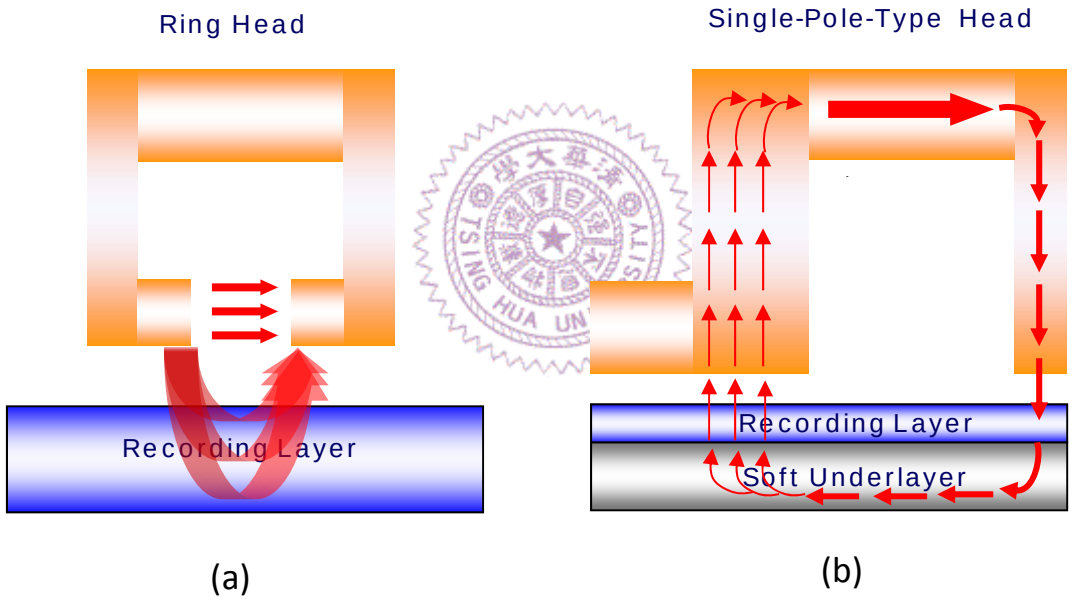

Figure 2- 3 Writing Process in (a) longitudinal and (b) perpendicular recording

In longitudinal recording, the ring head generates the field and the fringing field is used for writing the information. In the perpendicular recording, the main pole shoots magnetic flux across the recording layer. The magnetic flux comes back from the soft underlayer and it would be completely closed without loss. Therefore, in perpendicular recording the media can be experienced higher writing field.

2.1.4 Required Magnetic Properties of High Density PMR [2]

1. High perpendicular anisotropy (K_u): The high K_u is needed in order to obtain a negative nucleation field. Since the demagnetization field of the perpendicular recording media is $4\pi M_s$, the magnetostatic energy would be $0.5H_dM_s=2\pi M_s^2$.In order to resist the effect of demagnetization, the material such as CoPtCr-SiO_2, FePt, and $[Co/Pt]_n$, with high magnetocrystalline anisotropy is needed. Figure 2- 4 shows the H_k, which is defined as $2K_u/M_s$, as a function of $4\pi M_s$ [3].

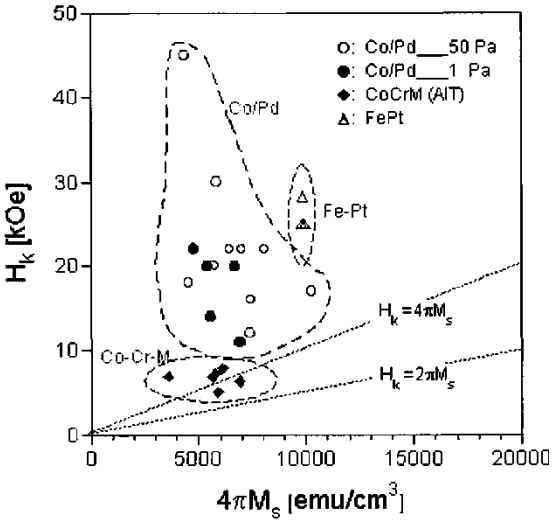

Figure 2- 4 Comparisons of the anisotropy field of various recording

Aside from this, the thermal stability is proportional to the K_u value. In general, the value of K_uV/k_BT, where V is the magnetic switching volume, k_B is the Boltzmann constant, and T is the absolute temperature, is required to be larger than 60 in order to keep the thermal stability of the media [4].

2. High coercivity (H_c): Theoretically, the linear density of a recording medium is proportional to the pulse width (PW_{50}). PW_{50} is measuring

the width of the signal pulse at 50% height and given by

$$PW_{50} = \sqrt{g^2 + 4(a+d)(a+d+\delta)}\,,$$

where g is the gap length, d is the magnetic spacing, δis the film thickness, and a is the transition parameter, which is expressed as

$$.a = \sqrt{\frac{4M_r\delta\left(d+\frac{\delta}{2}\right)}{H_c}}$$

In the above expression, M_r is the remanent magnetization of the medium. Therefore, higher H_c will result in small and sharp transition which is required in the high density PMR.

3. Uniform, small and isolated magnetic grains will increase the signal to noise ratio (SNR) and thermal stability.
4. Squareness (S), which is defined as M_r/M_s, close to 1 and a loop slope parameter (α value) near 1 are also favored magnetic properties. Figure 2- 5 shows the hysteresis loop with relevant parameters.

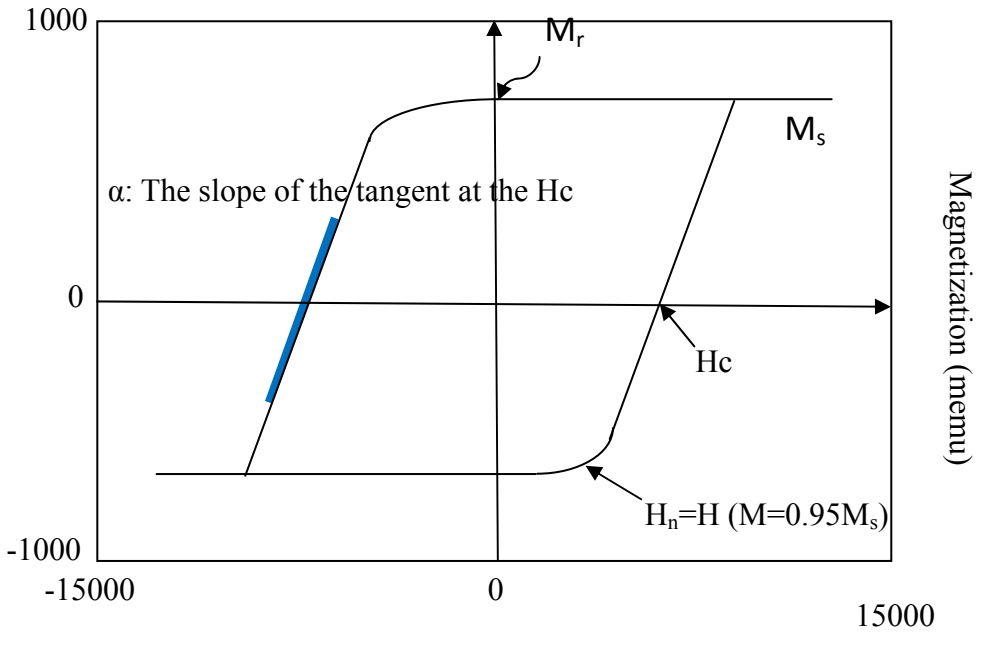

Figure 2- 5 The hysteresis loop of PMR with different parameters

2.2 Layer Structures of PMR

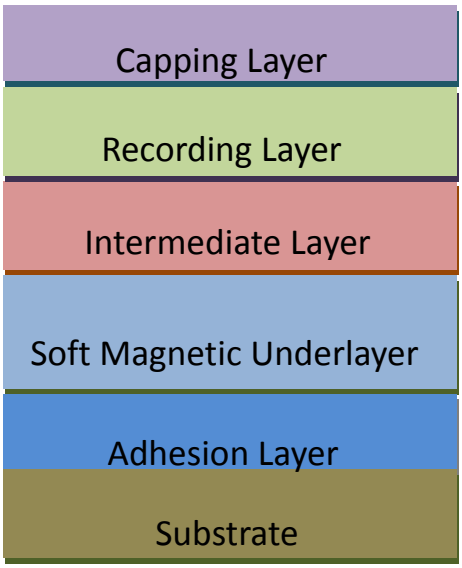

Figure 2- 6 The film structures of perpendicular recording medium

Figure 2- 6 shows the whole layer structures of the full-stacked perpendicular recording medium. The different functions of the different layers are discussed below.

2.2.1 Adhesion Layer

The substrate is first coated with an adhesion layer, made of Ta, Ti, or an alloy of these materials. This layer helps in improving the adhesion of SUL and all the other layers with the substrate.

2.2.2 Soft Magnetic Underlayer

This soft magnetic underlayer helps in conducting flux from the writing pole of the head to the trailing pole. In the writing process, the main pole

shoots magnetic flux across the recording layer and then come back to auxiliary pole through soft underlayer since the magnetization of the soft underlayer is in the in-plane direction. The magnetic flux could be completely closed, as shown in Figure 2- 3(b), and the writing fields would be greatly enhanced by the help of the soft underlayer. If the wirting fields are higher, the materials with higher Ku can be used as the recording medium. The grains can be smaller and stable in the recording medium with higher Ku materials, and the recording density can be further increased.

The noise from the soft underlayer is the main problem. Because the magnetization of the soft underlayer is much larger than the magnetization of the recording layer, the signal from the soft underlayer becomes the noise to the signal from the recording layer. Some materials such as CoTaZr, CoNbZr, FeAlSi, NiFeNb, FeTaC, FeTaC(N), CoFeB, FeAlN, etc., have been tried to solve this problem [5][6][7][8][9][10].

2.2.3 Intermediate Layer

On the top of the soft underlayer, the intermediate layers are deposited with or without the seed layers. The intermediate layers have two main functions. One is exchange-decoupling the SUL and the recording layer. A larger noise may be showed if the soft underlayer and the recording layer are coupled.

Another function is to provide epitaxial growth conditions for the recording layer. For example, for the perpendicular media with Co-based recording layers, to obtain grains with a Co [0002] orientation perpendicular to the film plane is necessary. Therefore, the intermediate

layer should have a face-centered-cubic (fcc) [111] orientation or a hexagonal close packed (hcp) [0002] orientation perpendicular to the film plane, as shown in Figure 2- 7 [2]. Table 2.1 summarizes some materials for the intermediate layers and their corresponding recording layers.

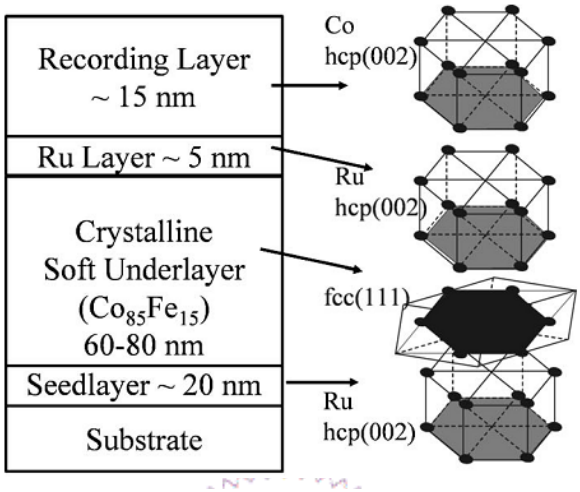

Figure 2- 7 Illustration of epitaxial growth of Ru and recording layer on fcc structure [2]

Table 2. 1 List of the intermediate layers and the recording layers

Intermediate layer	Corresponding Recording layer
Sc, Ti, Y, Re, Ru, Ge, etc. [11]	CoCr
Ti, CoNbZr [6]	CoCrPtNb
TiCr/$CoCr_{10}$ [12]	CoCrPt
TiCr [13]	CoCrPt
$CoCr_{35}$/TiCr [13]	CoCrPt
CrTi [14]	CoCrPt(Ta, B)
Ta, ITO [15]	Co/Pd
Ti [16]	CoCr
Ru [17]	CoPtCr-SiO_2

2.2.4 Recording Layer

Perpendicular recording media are widely studied such as CoCr-based, FePt, and $[Co/Pd]_n$ or $[Co/Pt]_n$ multilayer. The comparisons of these different recording layers are shown in Table 2.2 [18]. In this thesis, we will focus on the performance of the PMR with CoPtCr-SiO_2 recording layer. The addition of Pt can increase Ku value by the help of epitaxial growth. Cr segregation to the grain boundary can reduce the exchange coupling between the magnetic grains. SiO_2 will segregate at the grain boundary effectively at room temperature and it will also help to reduce the exchange coupling between grains. Thus, the well-isolated grain structure with large Ku value can be fabricated at room temperature.

Table 2. 2 Comparisons of different perpendicular media [18].

	Advantages	Disadvantages
CoCr-based	♦ Suitable for the recent recording mechanism	♦ Lower Ku and Hc than others ♦ Segregation and thermal stability needed to be improved
FePt	♦ High Ku and Hc ♦ High Ms ♦ Potential of future development	♦ High ordering temperature of process ♦ Large grain size about 40nm ♦ High exchange coupling ♦ Large demagnetization
$[Co/Pd]_n$ $[Co/Pt]_n$	♦ Higher Ku and Hc ♦ Potential of future development	♦ Difficult process for multilayer ♦ Large grain size and bad SNR

2.2.5 Capping Layer

The disk will be coated with carbon overcoats and lubricants to prevent the disk from failures caused by chemical reactions or mechanical impacts.

2.3 Magnetic Recording Layer and Intermediate Layer

2.3.1 Granular CoPtCr-SiO_2 Recording Layer

The Addition of SiO_2 to CoPtCr [19]

A well-isolated fine-grain structure with large perpendicular magnetic anisotropy, K_u, is strongly required for CoCr-based perpendicular media in order to achieve low media noise and high thermal stability. In 2002, T. Oikawa indicated that the addition of SiO_2 to CoPtCr is very effective to realize well-isolated fine-grain structure without disturbing the epitaxial growth of CoPtCr grains on Ru unerlayer. Figure 2- 8 shows the high-resolution TEM image of 16nm CoPtCr-SiO_2 recording layer. Fine grains and very thick amorphous-like grain boundaries are clearly observed. The lattice images of the sixfold symmetry are clearly seen for all grains, indicating good c-axis orientation of the grain normal to the film plane.

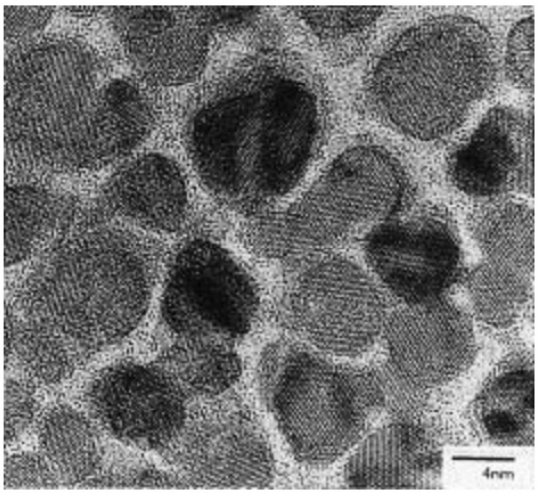

Figure 2- 8 High-resolution TEM image of 16nm thick CoPtCr-SiO_2 magnetic layer [19]

The values of K_u for CoPtCr-SiO_2 media with the thickness of more than 16nm are greater than $4x10^6$ erg/cm^3, which are almost twice as large as those of CoPtCr media as shown in Figure 2- 9. In Figure 2- 10, the dependences of Hc and M_r/M_s of the media shown in Figure 2- 9 are shown. The values of H_c of CoPtCr-SiO_2 recording media with the thickness of more than 12nm are larger than 4 kOe, which are much larger than the conventional perpendicular media without oxide segregation such as CoCrPt and CoCrPtB.

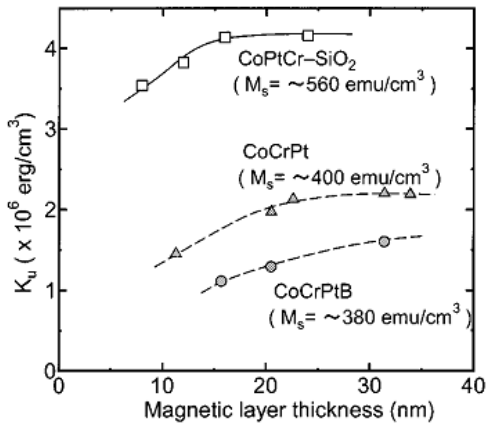

Figure 2- 9 Dependence of K_u of the CoPtCr-SiO_2 media on the magnetic layer thickness [19]

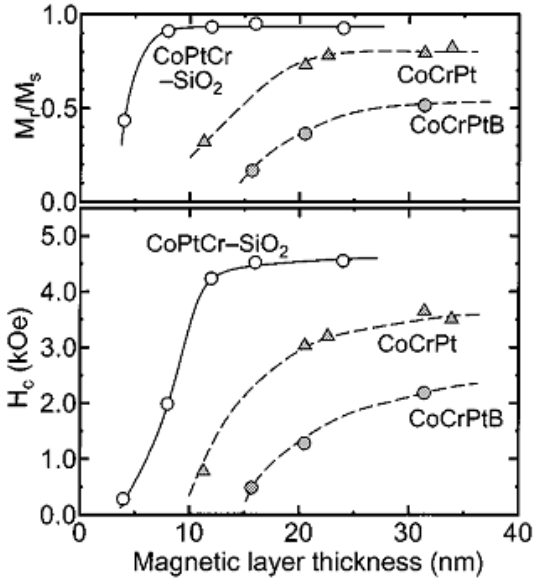

Figure 2- 10 Dependence of Hc and M_r/M_s of the CoPtCr-SiO_2 media on the magnetic layer thickness [19]

Optimization of the SiO_2 Content in CoPtCr-SiO_2 [20]

In 2004, Y. Inaba indicated that there was a tradeoff to be made between the thermal stability and media noise performance as a function of SiO_2 composition. The Hc of $\{[Co_{90}Cr_{10}]_{80}Pt_{20}\}_z$-$(SiO_2)_z$ media increased significantly as the SiO_2 content increased and exhibited a maximum of H_c at about 11at% SiO_2, i.e. 30 vol% SiO_2, as shown in Figure 2- 11.

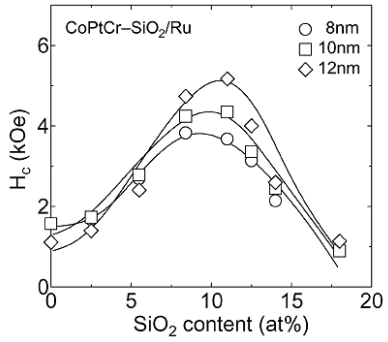

Figure 2- 11 Values of coercivity H_c as a function of SiO_2 content for CoPtCr-SiO_2 media with various film thickness [20]

Once the content of SiO_2 excesses 11%, the thermal stability will be degraded, resulting in lower Hc values. The TEM bright field images of CoPtCr-SiO_2 media with different SiO_2 contents as shown in Figure 2- 12. As the SiO_2 content increases from 0 to 14.4at % (~36 vol %), the grain diameter decreases apparently from 8.8 to 5.4nm. The K_u also decreased with increasing the SiO_2 content, as shown in Figure 2- 13. Thus, the decreasing of thermal stability (K_uV/k_BT) is probably due to the reduction of D_{grain} and K_u, which illustrated in Figure 2- 14.

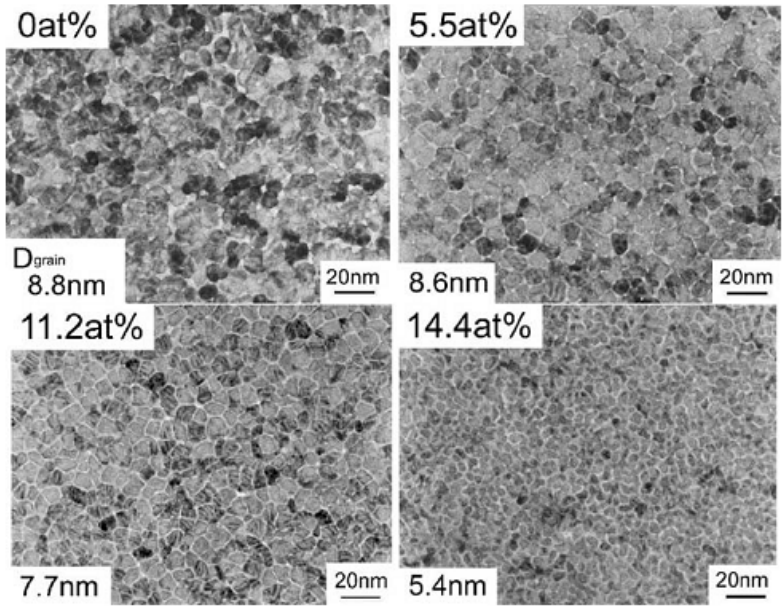

Figure 2- 12 TEM bright field images of CoPtCr-SiO_2 media with various SiO_2 contents [20]

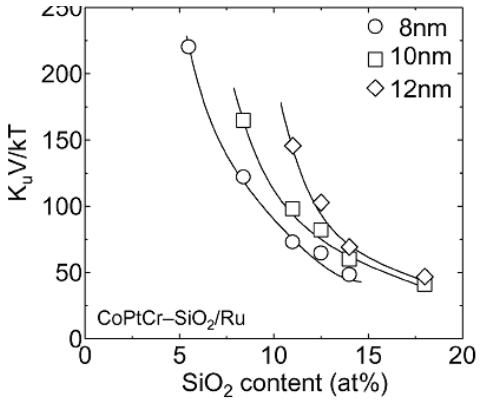

Figure 2- 13 Values of K_uV/k_BT as a function of SiO_2 content for media with various film thickness [20]

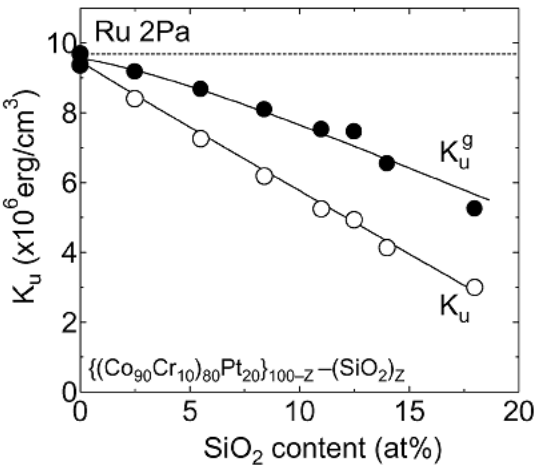

Figure 2- 14 Values of K_u for $\{[Co_{90}Cr_{10}]_{80}Pt_{20}\}_{100-z}$-$(SiO_2)_z$ media as a function of SiO_2 content [20]

Oxygen Effect on the CoCrPt and CoPtCr-SiO_2 Recording layer

In 1994, Takashi HIKOSAKA showed that the addition of oxygen was able to increase the perpendicular coercivity of CoPt film[21]. For films deposited under high working pressure, oxygen segregated at the grain boundary effectively, as shown in Figure 2- 15. The segregation of oxygen greatly reduced the intergranular magnetic interactions so as to increase the coercivity of the film, and the signal-to-noise (SNR) ratio can be promoted.

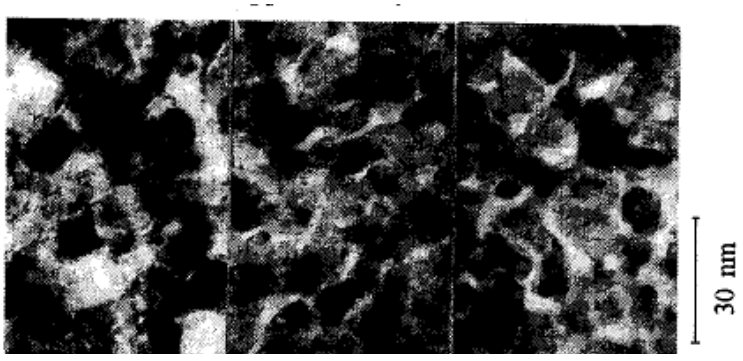

Figure 2- 15 TEM bright field images of CoPtO films. Oxygen to Co average content ratios were (a) 6.7% (b) 14% (c) 24% [21]

In 2000, Soichi Oikawa said that the addition of Cr to CoPtO film further decreased the exchange coupling between grains[22]. The CoPtCrO layer was deposited by sputtering the CoPtCr alloy target with oxygen reactive sputtering.Figure 2- 16 showed the TEM bright field image of CoPtCrO recording layer. It was found that both Cr and O segregated at the grain boundary. Furthermore, Co was also found at the grain boundary so the exchange coupling between grains was not to reduce acutely and the coercivity increased apparently.

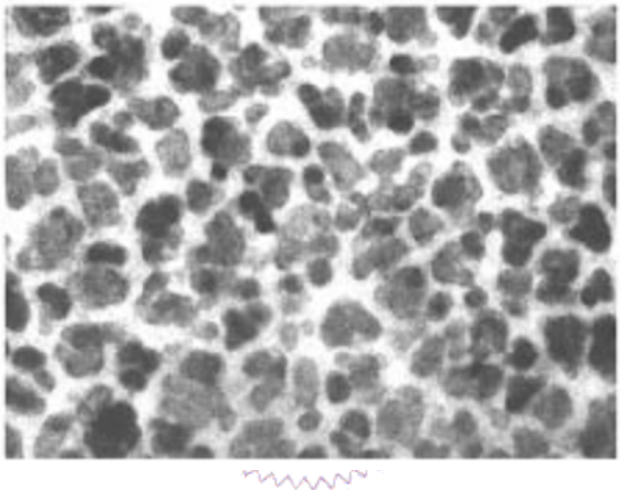

Figure 2- 16 The TEM bright field image of CoPtCrO magnetic layer**[22]**

In 2004, M. Zheng investigated the effect of oxygen on the perpendicular recording medium with CoCrPt-SiO_2 recording layer[23]. The recording layer was deposited by dc-magnetron sputtering in an Ar/O_2 mixed gas. Figure 2- 17 showed the TEM bright field images with different oxygen concentration in the mixed gas. Increasing the oxygen concentration could increase the grain boundary and decrease the grain size. The grain size decreased from 9.5nm to 4nm with increasing oxygen concentration from 10 to 21 at%.

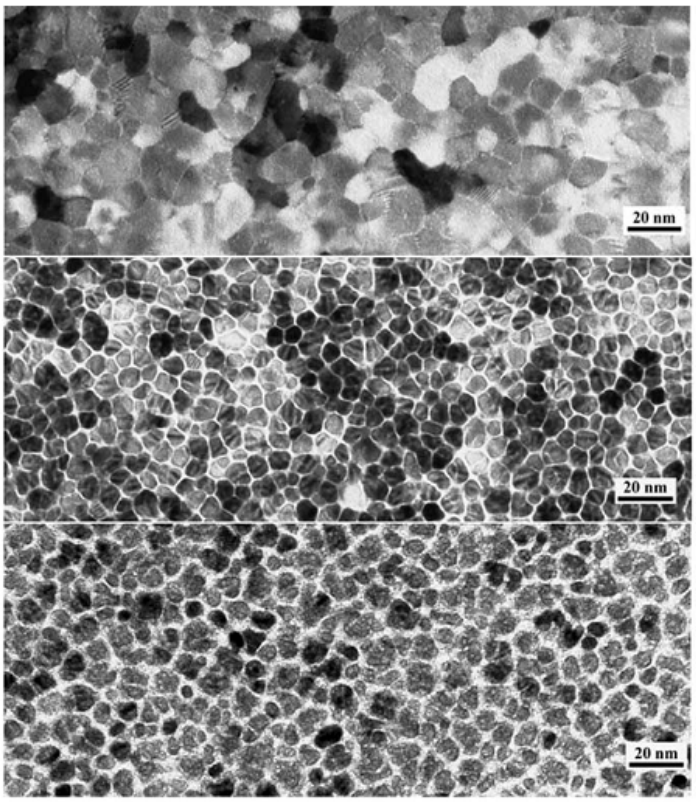

Figure 2- 17 TEM images for the media with 10 (top), 15(middle), and 21(bottom) at% oxygen[23]

The coercivity and saturation magnetization as functions of oxygen contents in the mixed gas were showed in Figure 2- 18. Zone I, where the content of oxygen was smaller than 15 at%, the coercivity increased with increasing the oxygen contents and the saturation magnetization remained constant. The adequate oxygen contents promoted Cr-O formation in the grain boundary. Thus the coupling between the grains was properly reduced and the coercivity was promoted. Zone II, where the content of oxygen was larger than 15%, both of the coercivity and the saturation magnetization decreased with increasing the oxygen contents. The decreased coercivity and saturation magnetization were caused by the excess oxygen in the core of the grains. To sum up, the optiumu oxygen contents was needed to improve the magnetic properties properly.

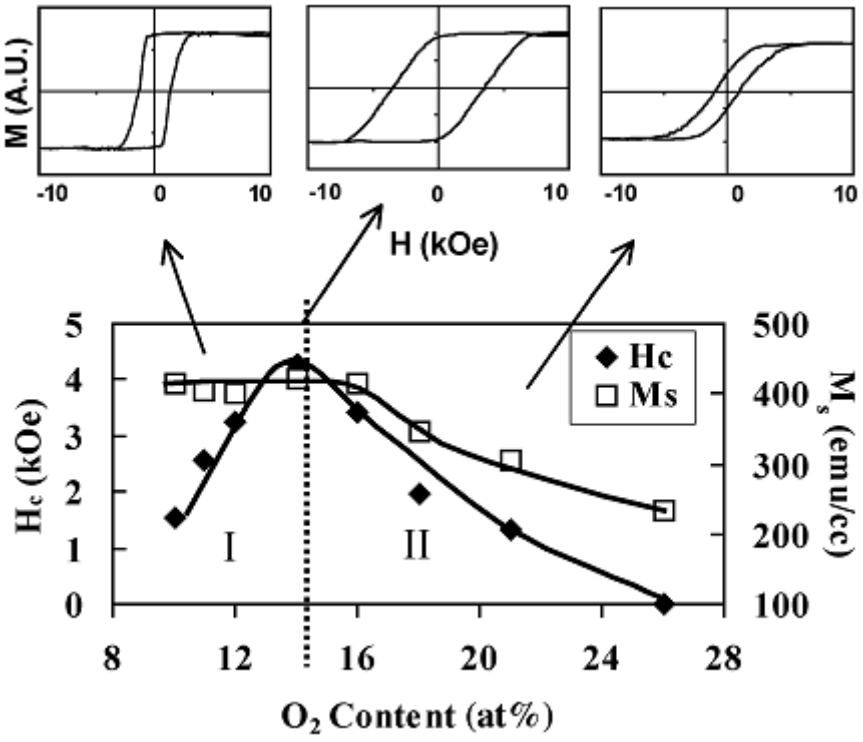

Figure 2- 18 Hc and Ms dependence on oxygen content for Co-Cr-Pt-Si-O PMR media. Selected VSM hysteresis loops are shown as well.[23]

In conclusion, Co-based granular medium which shows better magnetic properties, high anisotropy constant K_u and excellent SNR performance with good thermal stability possess the greater potential for high-density perpendicular recording media.

2.3.2 Intermediate Layer

Single Ru Intermediate Layer [17]

One of the main functions of the intermediate layer is to provide an epitaxial growth condition of the recording layer. In the CoPtCr-SiO_2 granular-type media, Ru is commonly used as an intermediate layer since

Ru and CoPtCr have the same crystal structure and similar crystal lattice parameters. The in-plane lattice paremeters, a, of Ru and Co are about 0.2705nm and 0.2503nm, respectively. The out-of-plane lattice constants, c, of Ru and Co are about 0.4281nm and 0.4060nm, respectively. The magnetic properties of CoPtCr-SiO_2 strongly depend on the sputtering condition of Ru intermediate. For example, as shown in Figure 2- 19, the coercivity enhance from 2.2 to 3.7 kOe merely by increasing the sputtering pressure of Ru intermediate layer from 5 to 20 mTorr. Figure 2- 20 displays that the surface roughness of the Ru layer increased with increasing the working pressure, which means that an increase of the coercivity in the recording layer due to enhanced domain-wall pinning. The results show that the Ru intermediate layer can provide the epitaxial growth condition for the Co-based recording layer and the enough surface roughness to supply the nucleation sites of the recording layer and to help the SiO_2 segregation from the grain boundary of the CoPtCr-SiO_2 layer. Ru is the most suitable material for the intermediate layer of the Co-based recording media so far.

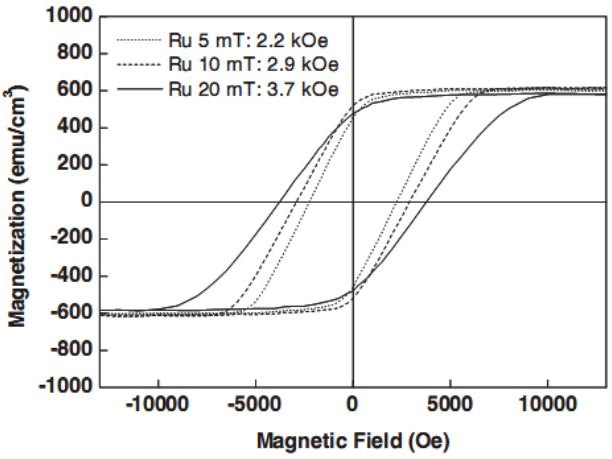

Figure 2- 19 Dependence of perpendicular hysteresis curves for samples with Ru layers deposited at 5, 10, and 20mTorr

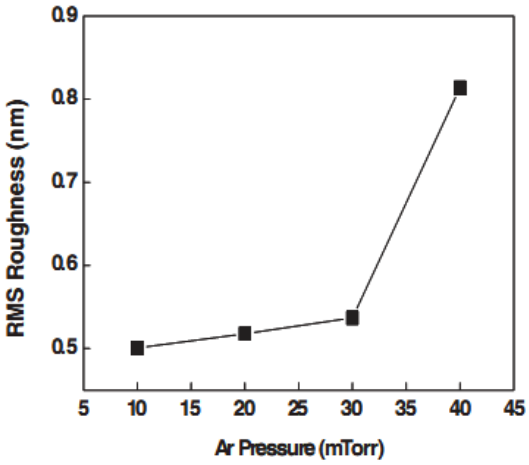

Figure 2- 20 Suface morphologies of the Ru films deposited at different working pressure

Dual-Ru Intermediate Layers [24][25][26][27][28]

For future high density recording, a reduction in the intermediate layer thickness is essential to improve the writability because the Ru underlayer is used as an interlayer between the recording layer and the soft-magnetic underlayer (SUL) [29]. However, the grains are less segregated when the Ru underlayer thickness is reduced. Therefore, the implementation of a thin Ru underlayer is difficult. A stacked Ru underlayer has been developed for the improvement of the microstructure of the recording layer with thin Ru underlayer. In the dual-stacked Ru underlayer (Ru#2/Ru#1), a layer of physically separated Ru grains (Ru#2) is grown on a layer of closely packed Ru grains (Ru#1), as shown in Figure 2- 21. The Hc and SNR of the media with the stacked Ru layer is higher than the media with the single Ru layer only, as shown in Figure 2- 22 and Figure 2- 23. In Co-based recording media, the texture of the intermediate layer and the surface roughness of the intermediate layer are both important. The good texture of the intermediate layer can promote the texture of the recording layer effectively, and the surface roughness of the intermediate layer can increase the nucleation sites of the recording layer so as to decrease the grain size of the recording layer. The grain size reduction can increase the signal-to-noise (SNR) ratio. It can't look after both sides in the single Ru intermediate layer, but it can be done in the dual-stacked Ru layer. The good texture is provided by the bottom Ru layer, and the surface roughness of the upper Ru layer is high. To sum up, the magnetic performance of the media with the dual-stacked Ru layer is better than it with single Ru layer if the thickness of the two intermediate layers is the same.

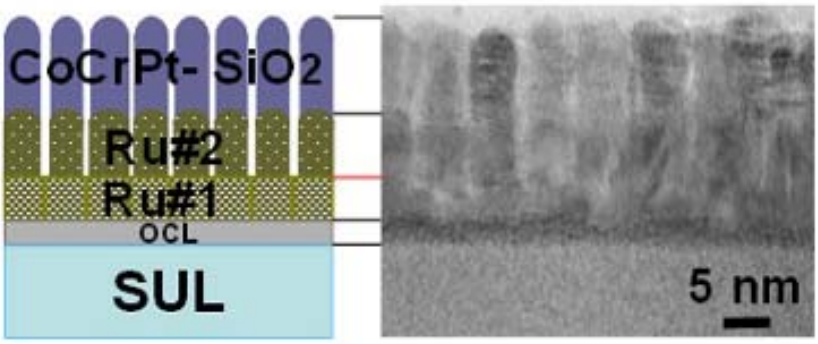

Figure 2- 21 Cross-sectional TEM image of a 16.7nm thick CoCrPt-SiO_2 magnetic film deposited on thin developed (Ru2/Ru1) underlayer of 11.9 nm thickenss [24]

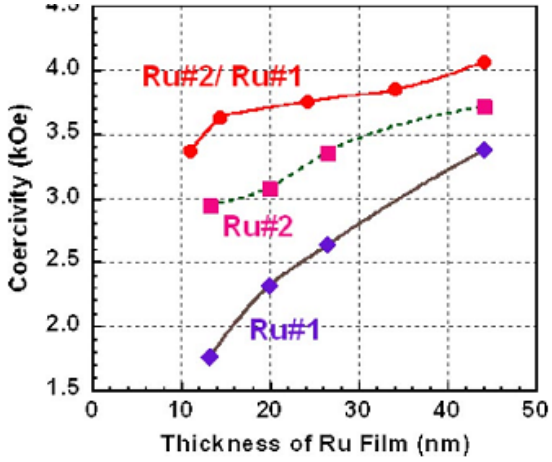

Figure 2- 22 Comparison of coercivity dependences on Ru underlayer thickness [24]

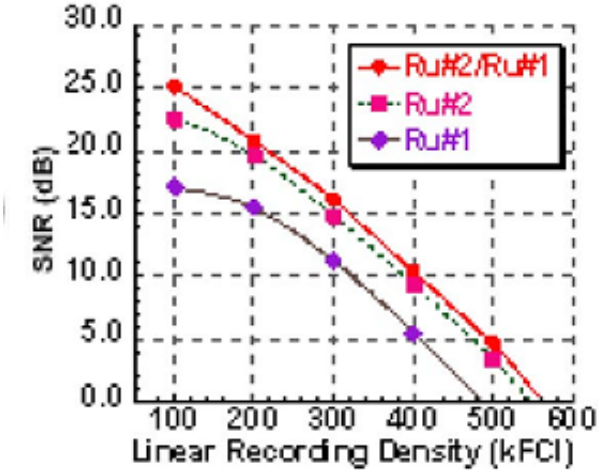

Figure 2- 23 Comparison of recording performance for monopole head of media with different Ru underlayer [24]

In 2007, S. N. Piramanayagam indicated that the grain size of the recording layer can be futher decreased by inserting a synthetic nucleation layer (SN layer) between the dual Ru layers. This layer consists of a monolayer or less of a suitable material as shown in Figure 2- 24. For suitable choice of materials and deposition conditions, this monolayer is expected to form dense nucleation sites due to the kinetics of the adsorbed atoms. Figure 2- 25 shows the TEM images of the upper Ru layer prepared without and with a SN layer, and Figure 2- 26 illustrates the grain size distribution of these layers. It can be seen that with the introduction of SN layer, the mean grain pitch is reduced by about 1nm to sub-6-nm and the grain size distribution also narrows.

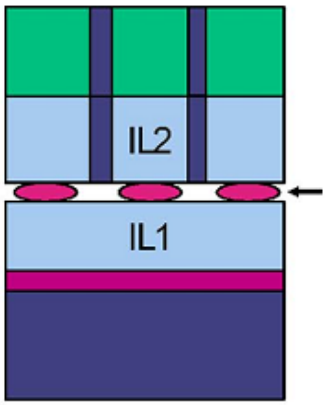

Figure 2- 24 Structure of perpendicular recording medium that uses nucleation control SN layer (indicated by arrow) [28]

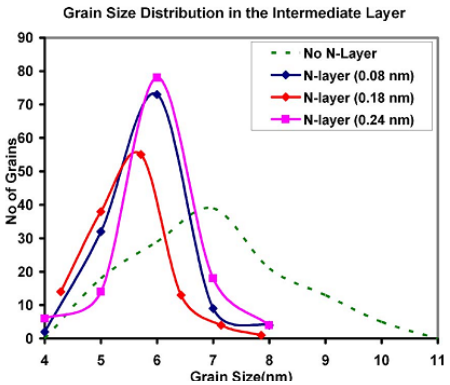

Figure 2- 25 Grain size distribution of the IL2 layer prepared without and with the nucleation control SN layer [28]

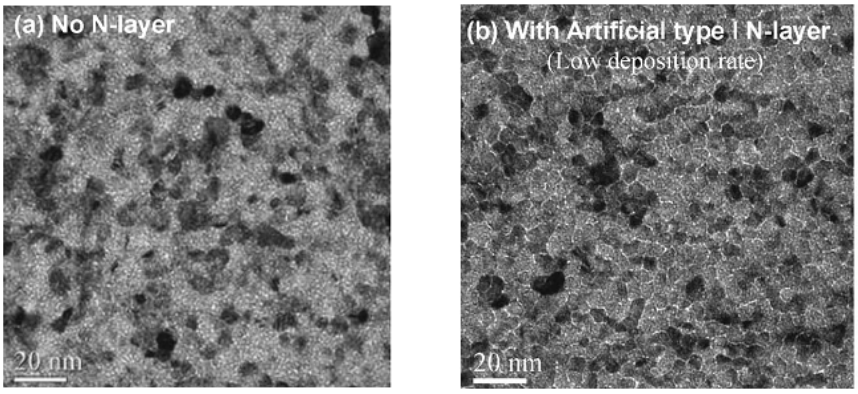

Figure 2- 26 Plan-view TEM images of the IL2 layer prepared

(a) without a SN layer, (b) with SN layer [28]

Ru/Ru-Oxide Interlayers [30][31]

Because grains in a CoPtCr-SiO_2 magnetic layer grown directly on the single Ru layer are not well isolated, particularly at the initial growth layer, a Ru/Ru-oxide interlayer combination was introduced to realize further intergranular exchange decoupling in the magnetic layer by forming Ru grains with small size and uniform distribution separated by nonmagnetic oxide phase grain boundaries. Figure 2- 27(a) shows the schematic of media layer structure and Figure 2- 27(b) shows the cross-section TEM image. In Table 2.3 are shown the magnetic properties of CoCrPtO media at various Ru thicknesses with and without Ru-oxide. The conclusion can be made that with the addition of a thin Ru-oxide layer on top of a Ru interlayer can further reduce the interlayer grain size while maintaining the vertical c-axis orientation and the grain clusters in the magnetic layer are well separated. A high Hc of 7000Oe can be obtained.

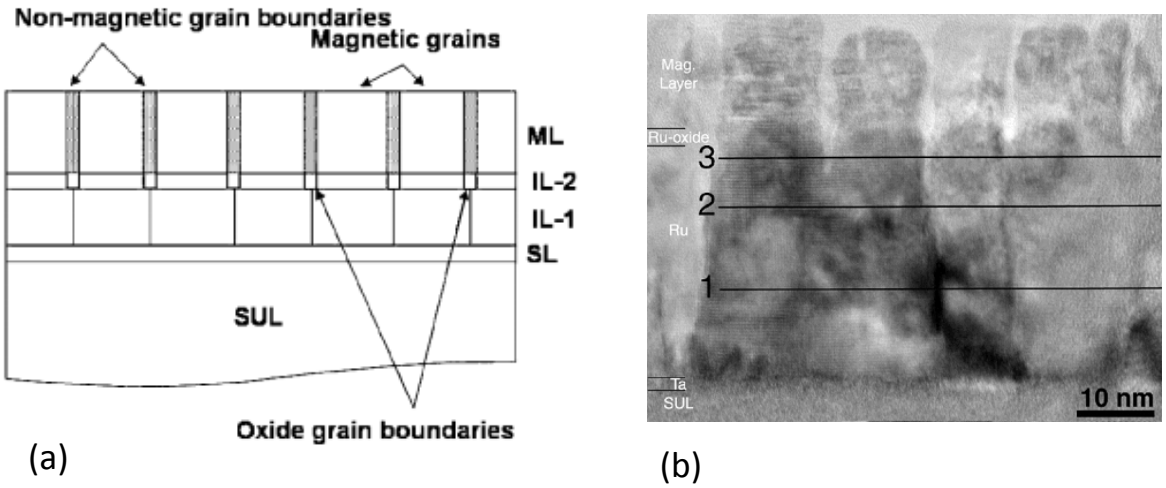

Figure 2- 27 (a) Schematic of media layer structure (b) Cross-section TEM image [30]

Table 2. 3 Magnetic properties of CoCrPtO media with Ru and Ru-oxide ILs [30]

Ru (nm)	Ru-oxide (nm)	H_c (Oe)	H_n (Oe)	S*	S
6	0	2400	-1940	0.78	1.00
6	2	4965	-2726	0.54	1.00
12	0	3964	-2350	0.59	1.00
12	2	5710	-2110	0.45	0.92
24	0	4572	-2425	0.58	0.91
24	2	6385	-2550	0.47	0.92
30	0	4756	-2930	0.63	0.97
30	2	6830	-3175	0.50	0.98

A RuCr alloy thin film deposited in an argon and oxygen reactive atmosphere was also studied as a grain size control layer for Co-based perpendicular recording medium. When the recording layer was deposited on such an intermediate layer, the grain size of the recording layer was about 6.4nm center-to-center distances. Figure 2- 28 shows the grain size distribution of CoCrPt-SiO_2 layers deposited on RuCr and RuCr oxide intermediate layers. It can be seen that the grain size can be reduced from 8nm to 6.4 nm when the media deposited on the RuCr oxide intermediate layer.

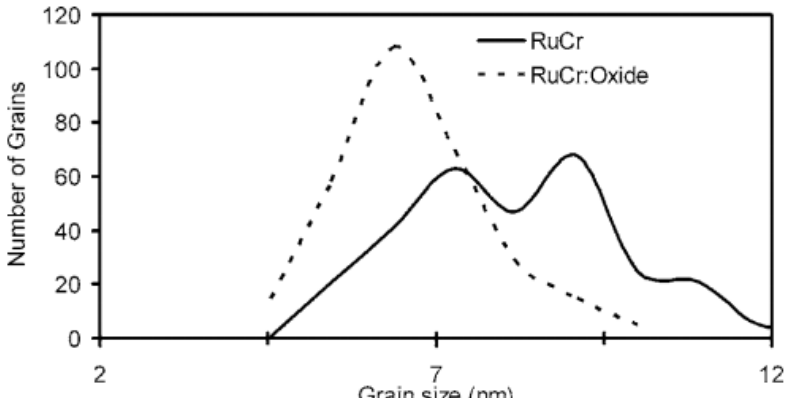

Figure 2- 28 Grain size distributions of Co grains in media deposited on $Ru_{90}Cr_{10}$ layers without oxygen and oxygen [31]

Alternative Materials for Ru Intermediate Layers [32][33]

Due to the need for high gas pressure in the sputtering of thick Ru layers, it is rush that an alternative to Ru be identified for this application. To obtain c-plane-oriented Co-base magnetic grains with a hexagonal close packed (hcp) structure by epitaxial growth on the nonmagnetic intermediate layer (NMIL), it is important to achieve precise control of both the wettability of magnetic grains on the NMIL and the lattice match between magnetic grains and the NMIL material. The NMIL face center cubic (fcc) based alloys were proposed by Atsushi Hashimoto in 2006[32], as these materials have a close packed atomic plane of (111) with sixfold-symmetric atomic arrangement. The highest value of coercivity (H_c) that was obtained for the Pt-Cr system with Sq=1.0 at 45at% Cr was 3.1 kOe, as shown in Figure 2- 29, and the coercivity increased with increasing the content of Cr in the Pt-Cr alloy up to the Cr concentration of 45at%. Figure 2- 30 shows cross-sectional TEM images and selected-area diffraction patterns (SADPs) of media with (a) Pt or (b) $Pt_{40}Cr_{60}$ NMIL. This result indicates that stacking faults (SFs) are formed parallel to the

(111) plane in the fcc Pt-Cr phase, resulting in streaks crossing the in-plane direction which are not apparent in the simple fcc phase [in Figure 2-30(a)]. Therefore, the enhancement in H_c by the formation of SFs in fcc NMILs is attribute to the preferred epitaxial growth of magnetic grains on the (111) terrace of the fcc NMIL due to collapse of the sixfold symmetry of the (111), (111) and (111) atomic terraces of the fcc NMIL, and the more appropriate NMILs for the Co-base recording media need to further study.

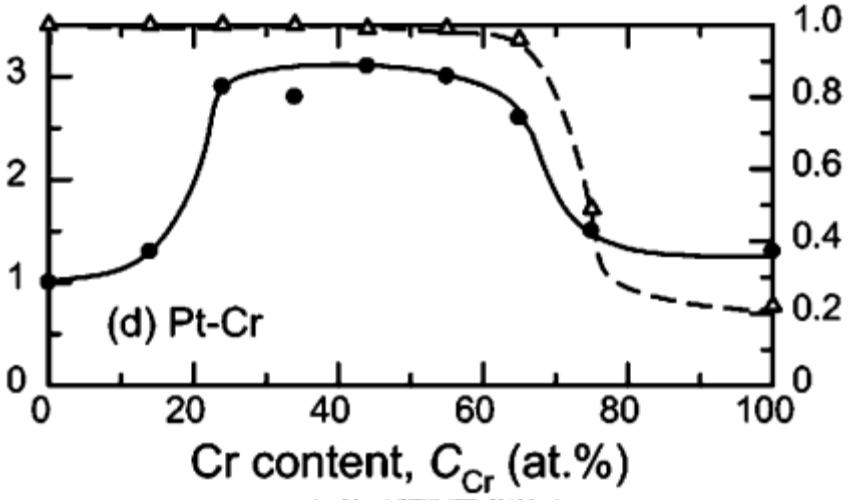

Figure 2- 29 Dependence of Hc (solid line) and Sq (broken line) on Cr content of NMIL with the recording media with Pt-Cr NMIL [32]

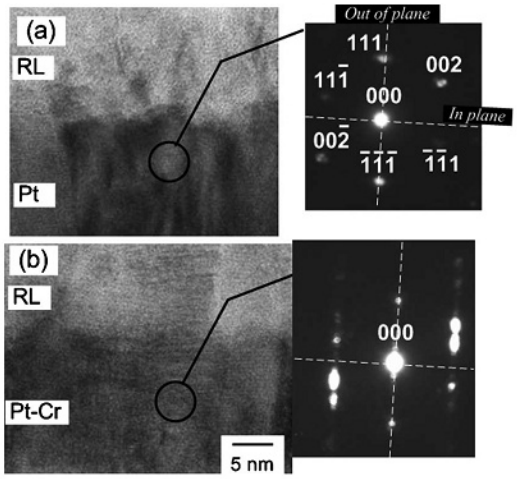

Figure 2- 30 Cross-sectional TEM images of the PMR films with (a) Pt and (b) Pt-Cr NMILs. Right figures show SADPs [32]

In the S. N. Piramanayagam's study [33], he proposed a metal intermediate layer (MIL) that can provide heteroepitaxial growth condition for the CoCrPt-SiO_2 layer. Figure 2- 31 shows the conventional intermediate layer structure and the new intermediate layer structure.

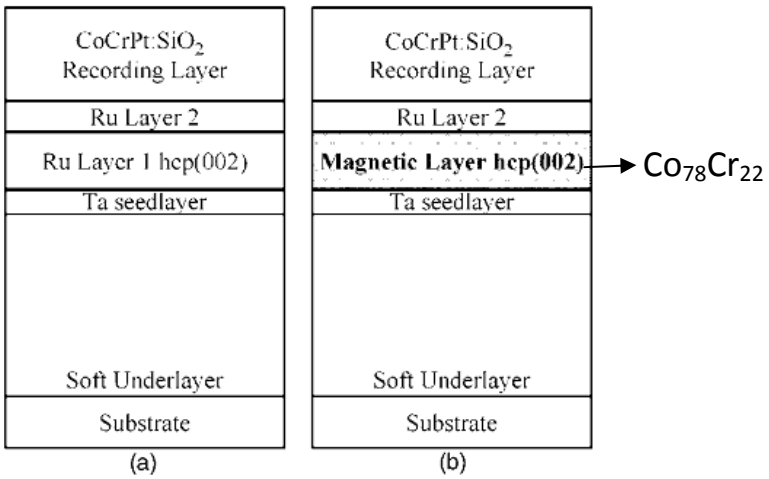

Figure 2- 31 Comparison of layer structures of recording media with (a) the conventional intermediate layer design and (b) the magnetic intermediate layer design [33]

Figure 2- 32 shows the coercivity of CoCrPt-SiO_2 recording medium with the CoCr underlayer and the $\triangle\theta 50$ of CoCrPt-SiO_2 recording layer. The coercivity increased with increasing the thickness of CoCr underlayer up to CoCr underlayer thickness of about 17nm. The $\triangle\theta 50$ of CoCrPt-SiO_2 recording layer decreased with increasing the thickness of CoCr underlayer. Figure 2- 33 shows the SNR and RMS of noise of the disks with magnetic intermediate layers. The exchange-breaking (EB) layer was inserted between the recording layer and the MIL to break the exchange coupling between the two layers. The increase of the SNR is significant up to an EB layer thickness of about 2.3nm. Similarly, the noise deceases with increasing EB layer thickness drastically until about 2.3nm. These results indicate clearly that the addition of the EB layer does help to reduce the noise and increase the SNR.

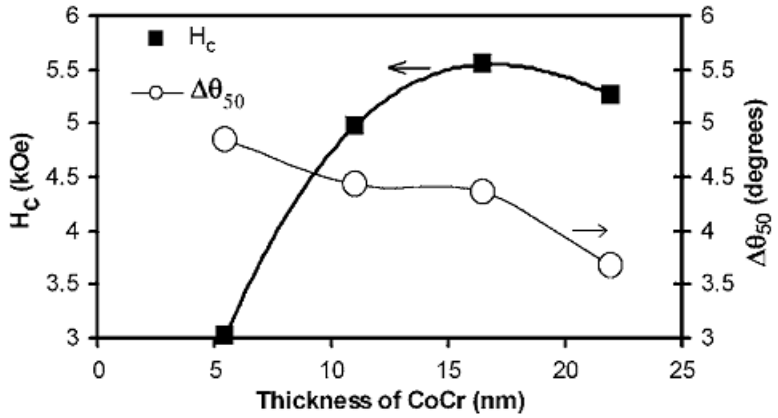

Figure 2- 32 Coercivity and △θ50 of hcp (00.2) peaks of CoCrPt-SiO_2 layers for different thicknesses of the CoCr intermediate layer [33]

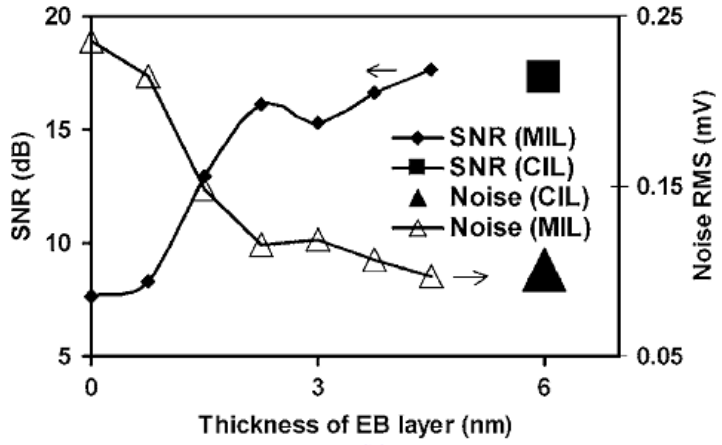

Figure 2- 33 Recording performance of CoCrPt-SiO_2 disks prepared on Ta/CoCr/Ru_1/Ru_2 with different Ru_1 layer thickness and Ta/Ru_1/Ru_2 intermediate layers (shown at the 6nm position in the x axis) [33]

In conclusion, the new intermediate layer structure which is suitable for the epitaxial growth condition for the Co-based recording layer is needed because of the high cost of Ru. The thickness of the intermediate layer also needs to decrease down in order to increase the writability of the recording media. There is still a lot of space to find the more convenient alternative intermediate layers.

2.4 The Origin of Noise of the PMR

2.4.1 The Soft Underlayer [34]

A significant amount of noise will be induced by an improperly optimized soft underlayer. The noise comes from the effective charges from the domain walls in the soft underlayer. To solve this problem, a magnetic biasing is added to the soft underlayer, as shown in the Figure 2-34. This biasing leads to complete saturation of the soft underlayer without domain wall inside.

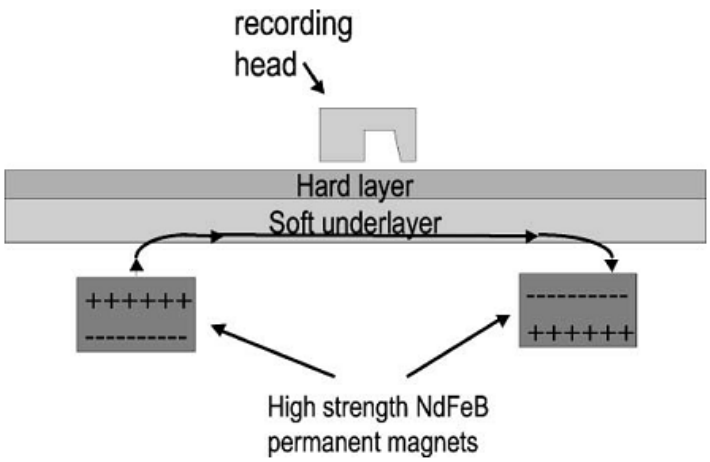

Figure 2- 34 A schematic of magnetic bias soft underlayer film [34]

The interlayer coupling between the recording layer and the soft underlayer also leads large noise. As mentioned before, the intermediate layer which is inserted between them can exchange-decouple the interactions. However, the thickness of the intermediate cannot be too large, or the magnetic flux back to the head will lessen.

2.4.2 The Recording Layer

A Noise Source Model for the Recording Layer [3]

As shown in Figure 2- 35, K. Ouchi et al., proposed a noise source model for a single layer perpendicular medium from the MFM observations in 2000. The noise amplitude, E_n, is expressed as:

$$E_n \propto d \times M_s \times \delta^{3/2} \times (1 - SQ)^{1/2},$$

where d is the reserved domain diameter, M_s is the saturation magnetization, δ is the film thickness, and SQ is the perpendicular squareness. The media noise is proportional to the domain size which attributes to the reversed domains that inevitable occur to compromise the magnetostatic energy. The large SQ and small domain diameter, d, will reduce the reversed domains. Therefore, large SQ and small domain diameter will enhance the SNR performance.

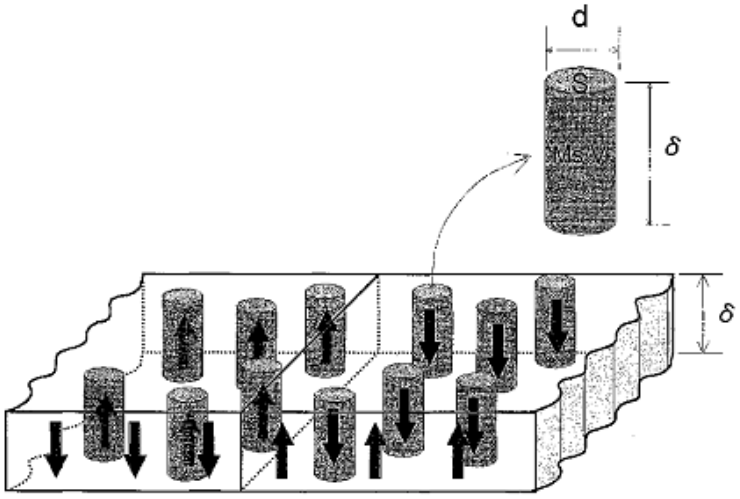

Figure 2- 35 Noise Source model for perpendicular recording media [3]

The Effect of Magnetic Cluster Size [35]

As shown in Figure 2- 36, the SNR decreases and the noise increases as increasing the linear density, especially magnified at larger magnetic cluster size. The larger cluster magnetic size contributes to the increase in the transition media noise so as to decrease the SNR.

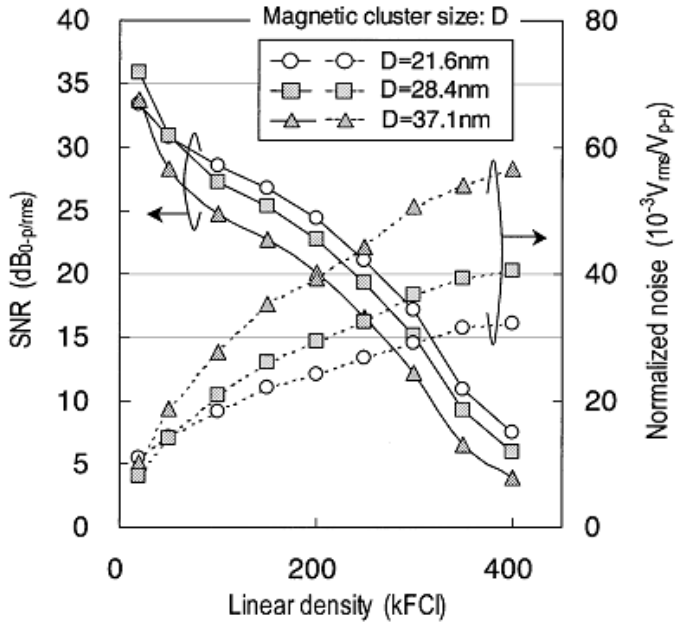

Figure 2- 36 Recording density dependence of SNR and normalized media noise [35]

Intergranular Coupling and Switching Field Distribution (SFD)[36][37][38]

Both the coupling between the grains in the recording layer and the switching field distribution (SFD) influence the SNR a lot. Therefore, it is an important issue to measure the intergranular coupling and the SFD. △M measurement is a widely used method to measure intergranular coupling by calculated by DCD curve and IRM curve. The SFD is obtained by the

differentiated DCD curve. In the DCD (dc demagnetization) measurement, the recording medium is initially negative magnetized, and then the remnant magnetization is measured. The remnant magnetization means the magnetization at the zero field after adding a small positive field. The remnant magnetization is measured as a function of increasing the positive applying field. In the IRM measurement, the remnant magnetization is also measured as a function of increasing the positive field but the initial magnetization state is an ac demagnetization state. According to the Stoner-Wohlfarth relation for non-interacting single domain particle [39], the remnant magnetization measured by these two methods can be expressed as:

$$M_{DCD}(H) = 1 - 2M_{IRM}(H).$$

In real case, there is some deviation and the deviation defined as $\triangle$M.

$$\Delta M \equiv M_{DCD}(H) - [1 - 2M_{IRM}(H)].$$

However, the H field in above equations should be expressed in the actual field, H_{tot}, instead of the external field, H_{ext}. The actual field includes the demagnetization field which would lead to broadening of DCD curves and IMR curves. The relation between H_{tot} and H_{ext} can be expressed as:

$$H_{tot} = H_{ext} - 4\pi NM\,, \qquad 0 \le N \le 1$$

N is the effective demagnetization factor. In René J. M. van de Veerdonk's study [37], they measured a perpendicular CoCrPt alloy medium with the

saturation moment Ms=315 emu/cm^3. Figure 2- 37(a) shows a series of recoil loop, and Figure 2- 37(b) shows the uncorrected, the corrected DCD curves and SFD. The uncorrected DCD curves consider the H_{ext} only. If we want to know the corrected DCD curve, we will need to know the H_{tot}, so we need to calculate the value of N. Consider the four equations showed below:

$$H_{tot,-\sigma} = H_{cr}\exp(-\sigma_{SFD})$$

$$H_{tot,+\sigma} = H_{cr}\exp(+\sigma_{SFD})$$

$$H_{tot,-\sigma} = H_{ext,sw1} - 4\pi NM_{sw1}$$

$$H_{tot,+\sigma} = H_{ext,sw2} - 4\pi NM_{sw2}$$

Where $H_{tot,+\sigma}$ and $H_{tot,-\sigma}$ are the fields where 16% and 84% of the magnetization has been irreversible switched. H_{cr} is the field where the remanent magnetization (Mr) is equal to zero. σ_{SFD} is the standard deviation of SFD. $M_{sw1,2}$ are equal to ±0.68 x $M_{sat,r}$, respectively. To solve the four equations mentioned above, σ_{SFD} and N can be expressed as:

$$\sigma_{SFD} = \ln(h_- + \sqrt{h_-^2 + \beta})$$

$$N = \frac{H_{cr}}{4\pi M_{sw2}} x(h_+ - \sqrt{h_-^2 + \beta})$$

where $h\pm=[H_{ext,sw2}\pm\beta H_{ext,sw1}]/2H_{cr}$, and $\beta=M_{sw2}/M_{sw1}$. The value of N can be calculated, and a new DCD curve can be obtained by replying the value

of N to the recoil loops. Repeat the iterative process until the value of N converges to a constant, and the DCD curve is the corrected one, as shown in Figure 2- 37(b). Figure 2- 37(b) also illustrates SFD that could be calculated by differentiating the corrected DCD curves.

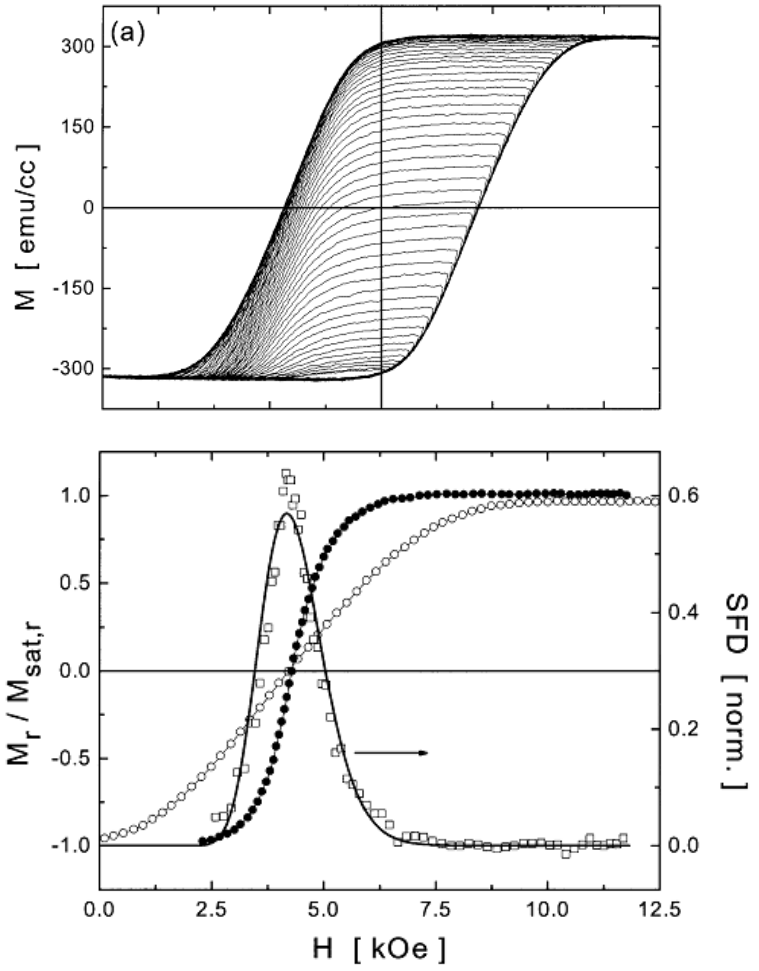

Figure 2- 37 (a) Example of a series of recoil loops measured on a CoCrPt alloy. (b) Normalized DCD remanence curves extracted from the recoil loops. The open ciucles and solid circles are represented the uncorrected and corrected DCD curves, respectively. The open square represented SFD.[37]

IRM curves can be obtained by the same method, but the initial states of the recoil loops are demagnetization state. The recoil loops, IRM curves and △M are shown in Figure 2- 38(a) and Figure 2- 38(b).

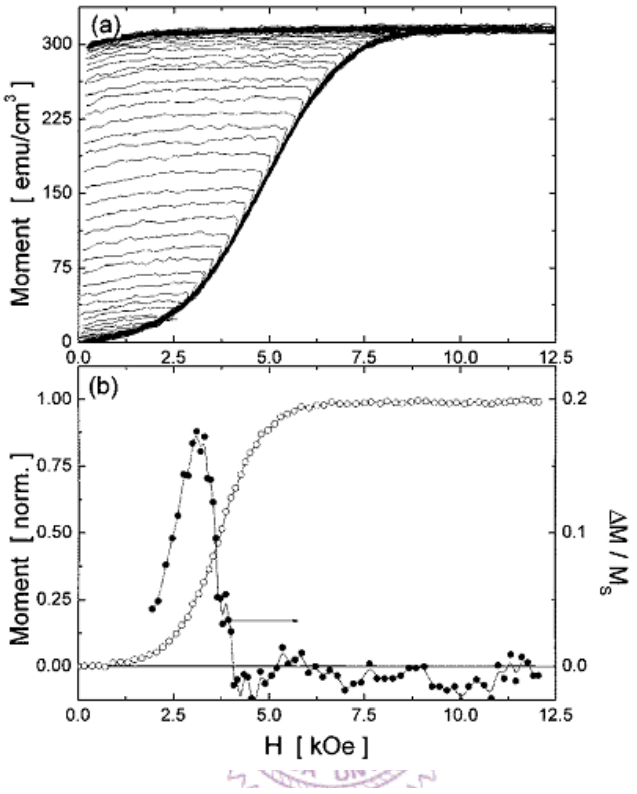

Figure 2- 38 (a) Examples of a series of recoil loops (b) The open circles represent IRM curve, and the solid circles represent △M of the perpendicular CoCrPt film mentioned above [36]

The value of N and σ_{SFD} of the perpendicular CoCrPt film mentioned above are 0.57 and 0.17, respectively. The value of △M of the CoCrPt film is positive, that means the exchange coupling between grains in the CoCrPt film are dominating. The △M and SFD for the CoCrPt films with different film thickness are also calculated[38]. Figure 2- 39 shows the △M as a function of the film thickness. The △M values decrease from the positive value to the negative value, that indicates the intergranular exchange

coupling is significantly reduced with increasing the film thickness. Figure 2- 40 shows the N factor and the σ_{SFD} as a function of △M.

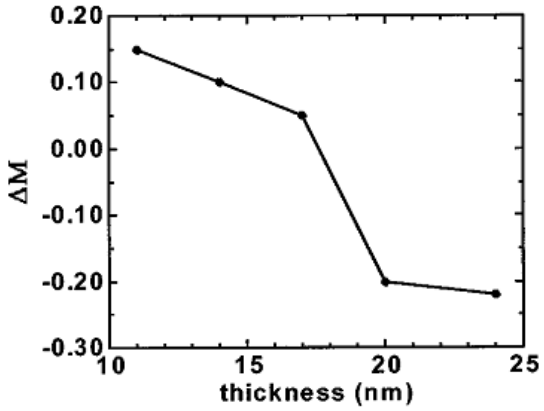

Figure 2- 39 Thickness Dependence of the △M for the CoCrPt Alloy[38]

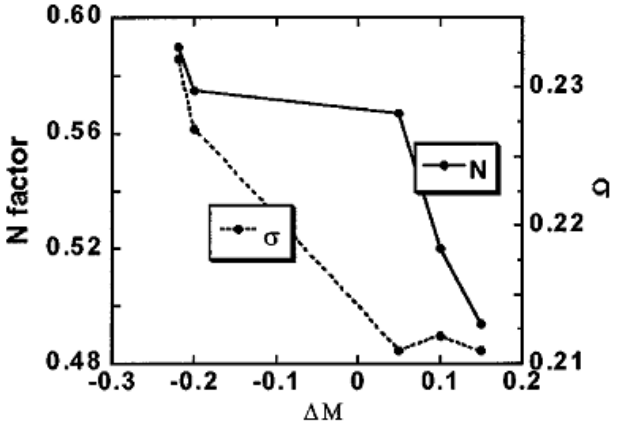

Figure 2- 40 △M dependence of the effective demagnetization factor (solid line) and the SFD (dashed line)[38]

In conclusion, we can use the △M measurement to measure the intergranular exchange coupling. The larger intergranular exchange coupling will lead to large media noise which is undesirable. The SFD can also be obtained by differentiating DCD curves. The narrower SFD is desirable to increase SNR. We can improve the PMR performance by using this measurement.

Chapter 3 Experimental

3.1 Experimental Flow Chart

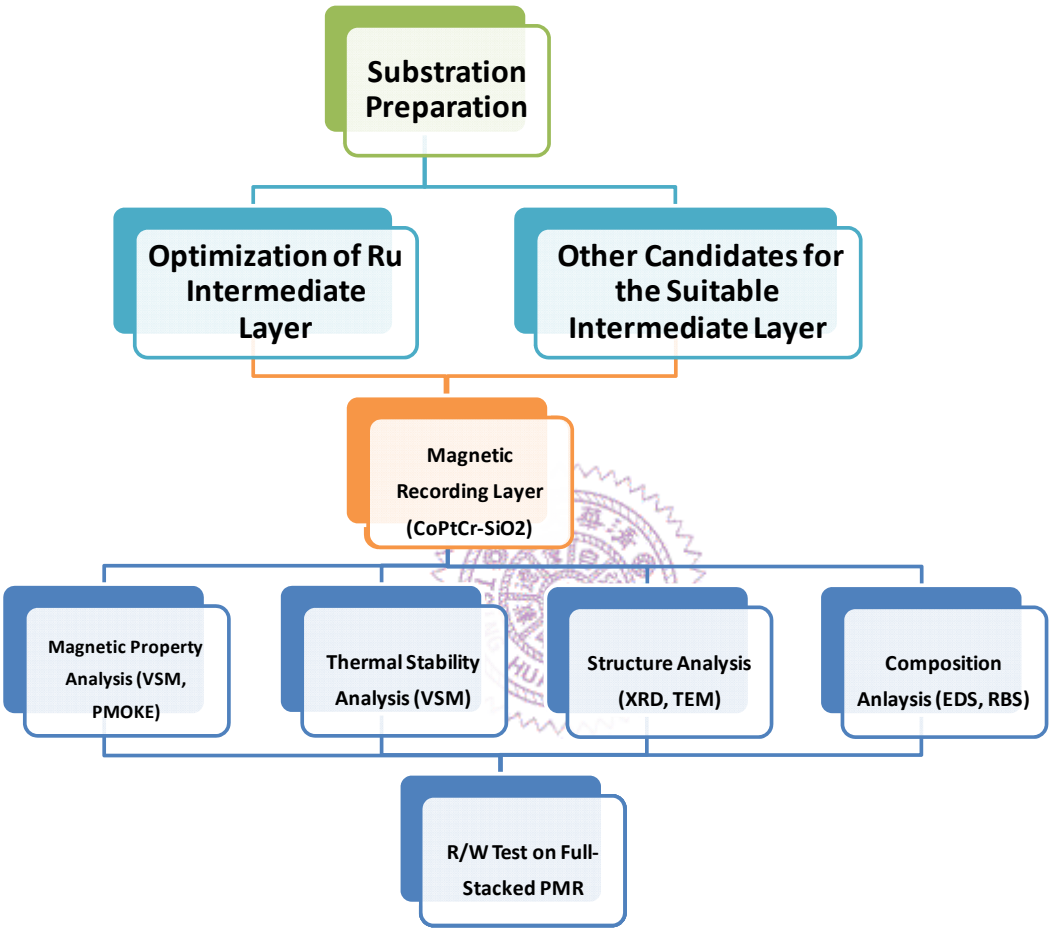

3.2 Ultra-High Vacuum Sputtering System (UHV)

The sputtering system is fabricated by ULVAC Corporation Taiwan. The system is composed of two chambers: one is the main chamber and another is the loading chamber as shown in figure. In the main chamber, there are four magnetic guns and four non-magnetic guns. The ultimate background

pressure is $5x10^{-9}$ Torr in the main chamber. In the loading chamber, there is the transfer manipulator that contains the single-axis gimbals and the transfer valve, as shown in figure. The ultimate background pressure is $1x10^{-7}$ Torr.

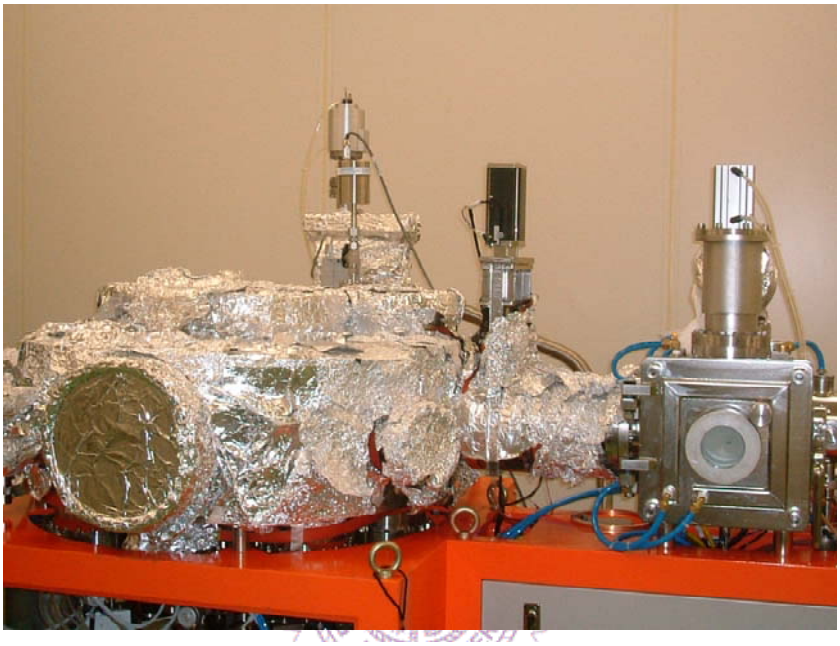

Figure 3- 1 The UHV sputtering system

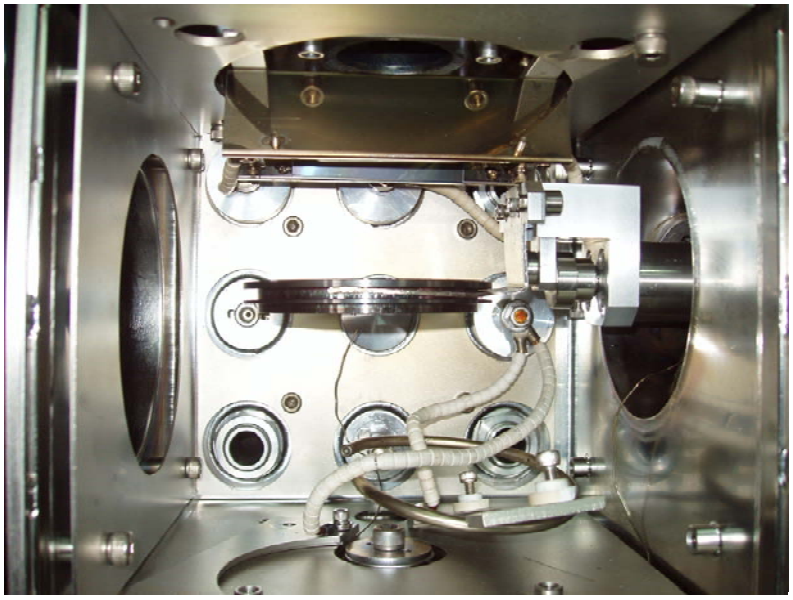

Figure 3- 2 The transfer manipulator in the loading chamber

3.3 Analysis Technique

3.3.1 Vibrating Sample Magnetometer (VSM)

The picture of VSM is shown in Figure 3- 3, and the scheme diagram of VSM is shown in Figure 3- 4. As shown in Figure 3- 4, during measurement, the measured sample vibrates in the direction perpendicular to the applied field together with the reference sample that is in the loudspeaker. The vibration of the measured sample will induce the electromotive force in the detection coils, and so as the reference sample. We can compare the electromotive force in the detection coils and it in the reference coils to know the magnetization of the samples since we have known the magnetization of the reference sample. This measurement was first proposed by Foner.

Figure 3- 3 The picture of VSM

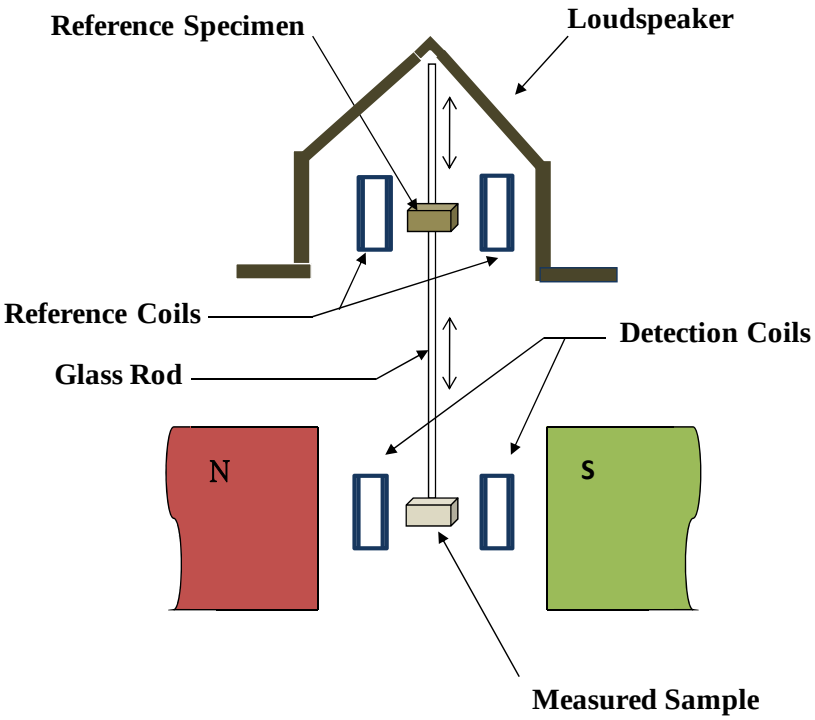

Figure 3- 4 The scheme diagram of VSM

3.3.2 Perpendicular Magneto-Optical Kerr Effect Meter (PMOKE)

Figure 3- 5 shows the scheme diagram of perpendicular magneto-optical Kerr effect meter (PMOKE). First the linear polarized He-Ne laser light is beamed the measured sample. Then, the magnetization of the sample will change the dielectric constant tensor of the sample form diagonal-only form to the non-diagonal form. The complex tensor will interact with the linear polarized light, and the reflect light from the sample will have the elliptical polarization. During the measurement, changing the applied field will change the direction of the magnetization and it will cause the different ellipticity of the polarization in the reflection light from the sample. The reflected light is guided into another linear polarizer and then into a photo-diode. The photo-diode voltage induced by the reflected light called Kerr intensity is proportional to the magnetization, and we can

measure the hysteresis loop by using this method.

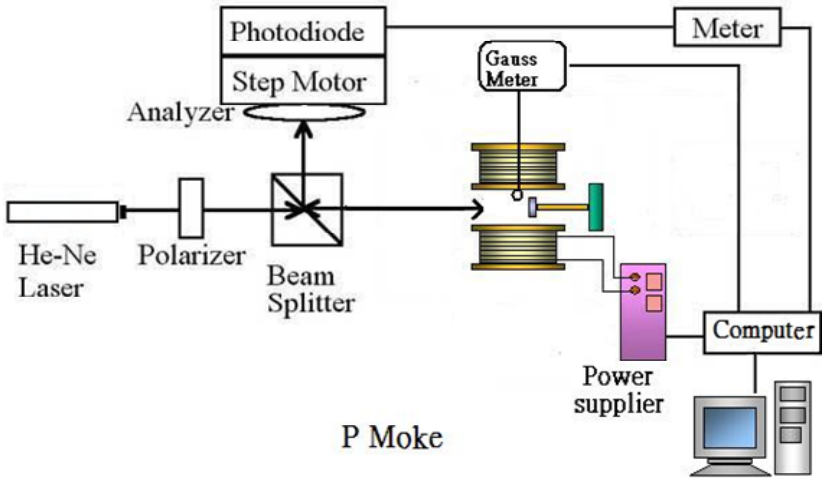

Figure 3- 5 The scheme diagram of PMOKE

3.3.3 Atomic Force Microscopy (AFM)

The atomic force microscope (AFM) is a relatively new tool for measuring intermolecular forces between nanometer-scale objects. The type of this apparatus is DI3100. Tapping Mode is usually used to simulate the roughness and film thickness. An atomically sharp tip is scanned over a surface with feedback mechanisms that enable the piezo-electric scanners to maintain the tip at a constant force to obtain height information above the sample surface. Figure 3- 6 shows the sketch of AFM. The nanoscope AFM head employs an optical detection system in which the tip is attached to the underside of a reflective cantilever. A diode laser is focused onto the back of a reflective cantilever. As the tip scans over the surface of the sample, the laser beam is deflected of the attached cantilever into a dual element photodiode. The photo-detector measures the difference in light intensities and then converts into voltage. Feedback from the photodiode

different signal enables the tip to maintain either a constant force or constant height above the sample, and the information about the surface of the measured sample can be obtained.

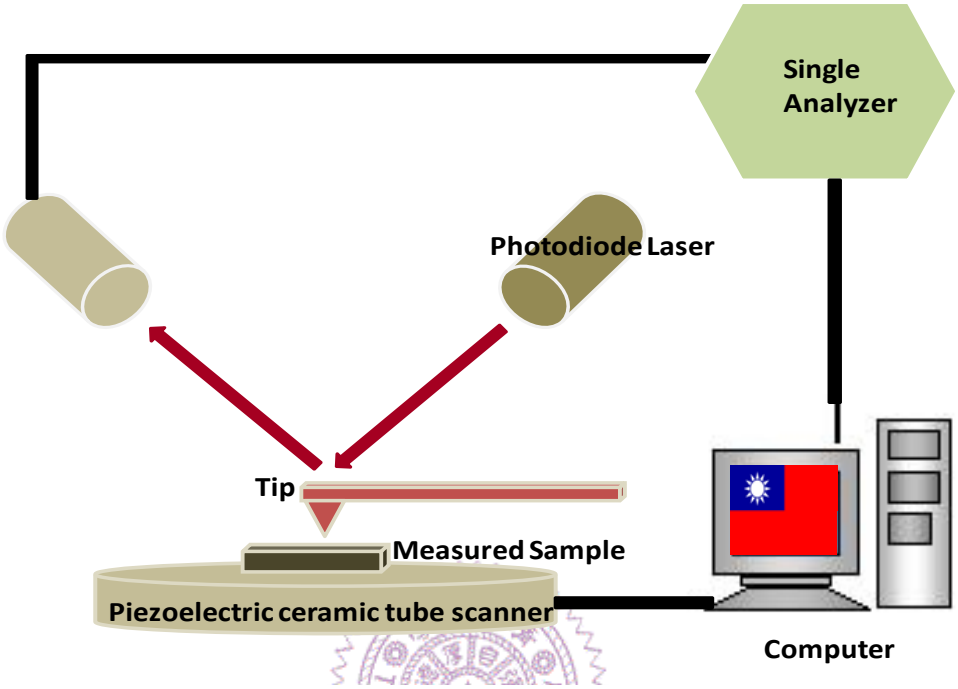

Figure 3- 6 The scheme diagram of AFM

3.3.4 X-Ray Diffraction (XRD)

Figure 3- 7 shows the sketch of XRD instrument. As shown in the Figure 3- 7, the rotating axis of the specimen and the detector are defined as θ and 2θ axis, respectively. The specimen is positioned so that its reflecting planes make some angle θ with the incident beam, and the detector is set at the corresponding angle 2θ. From the Bragg law, "$2d\sin\theta = n\lambda$", the lattice constants of the specimen can be obtained. It can used to determine about an unknown crystal by measurements of the directions of diffracted beams.

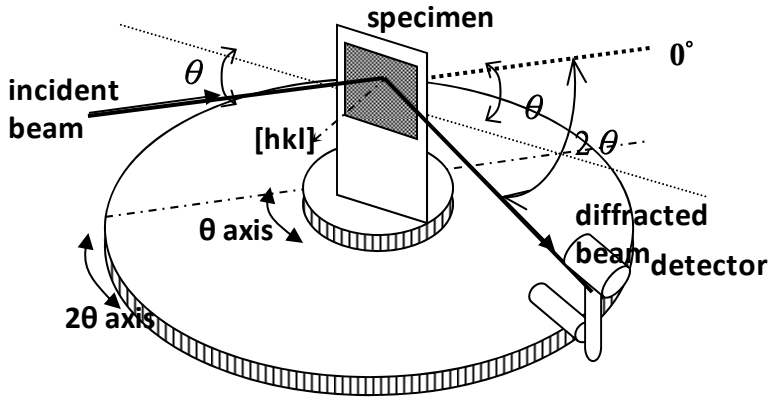

Figure 3- 7 The scheme diagram of XRD instrument

3.3.5 Transmission Electron Microscope (TEM)

The detail analysis of TEM comes from the diffraction of electrons from the crystallographic planes of the object being investigated. The source is an electron gun and the magnetic lenses are energized by direct current, being composed normally of a current-carrying coil surrounded by a soft iron case. The HRTEM is also equipped with EDX and EELS to analysis the stoichiometry of grains and grain boundary. Moreover, grain size, segregation state and whole film structure could be observed by the plane view and cross-sectional images.

3.4 Read and Write (R/W) Test

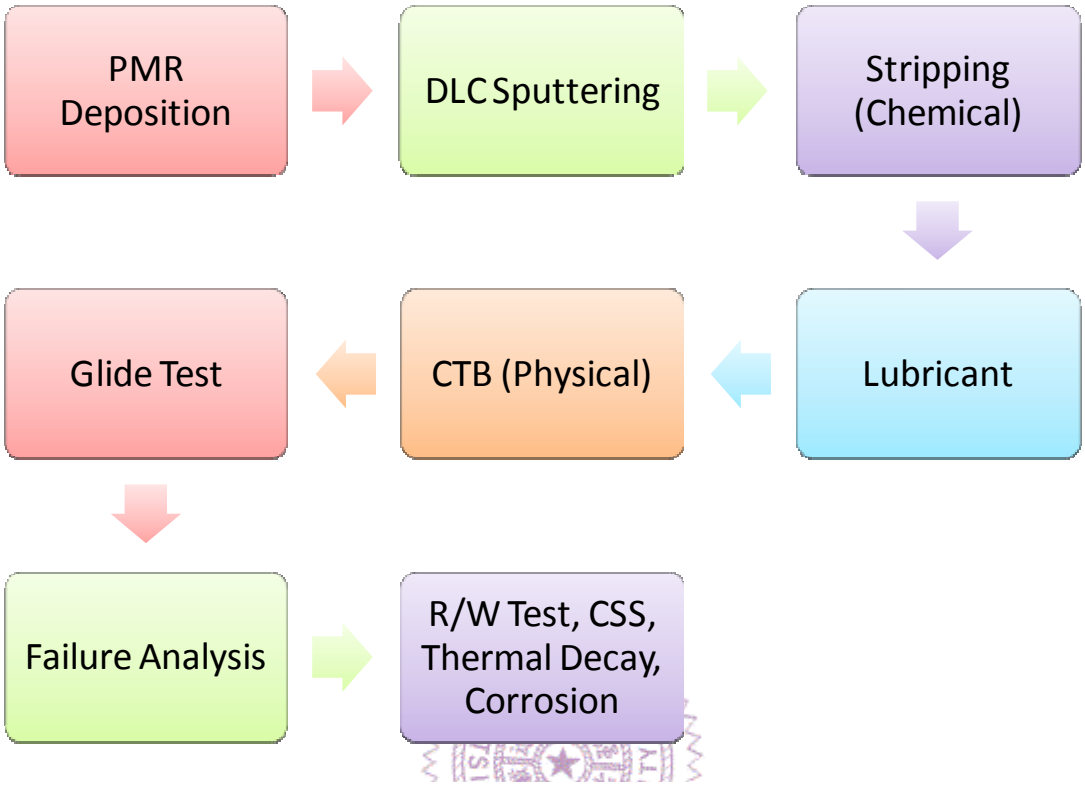

Figure 3- 8 Standard post-processing of commercial disk

Figure 3- 8 shows the standard post-processing of commercial disk. First, a very thin diamond like carbon (DLC) film about 4-5nm is deposited on the recording layer for oxidation free. The following process is to strip with chemical solution and to spin-coat a lubricant layer in order to prevent the contaminants upon the disk and prevent the disk directly contact with the MR head, respectively. The physical polishing process named CTB is used for removal the rest contaminants and the Glide Test is used for prominence examination. After finishing all processes, it is appropriate to carry out the Read and Write Test to obtain the signal-to-noise (SNR) ratio of our PMR films.

Chapter 4 Results and Discussion

4.1 Current Full-Stack Perpendicular Recording Media

The current Co-based perpendicular recording media in the previous study is shown in this section. The layer structure is: Ta 3nm/Pt 7nm/Ru 30nm/ CoPtCr-SiO_2 17.5nm/Ta 3nm. The θ-2θ XRD scans is shown in Figure 4- 1. We cannot distinguish Ru hcp(00.2) peak from Co hcp(00.2) peak. The hysteresis loop is shown in Figure 4- 2. The coercivity of this film is 4755Oe. The α, which is defined as $4\pi(^{dM}/_{dH})|_{H=Hc}$, was equaling to 1.94. The stronger exchange coupling between grains in the recording layer, the higher value of α that is undesirable.

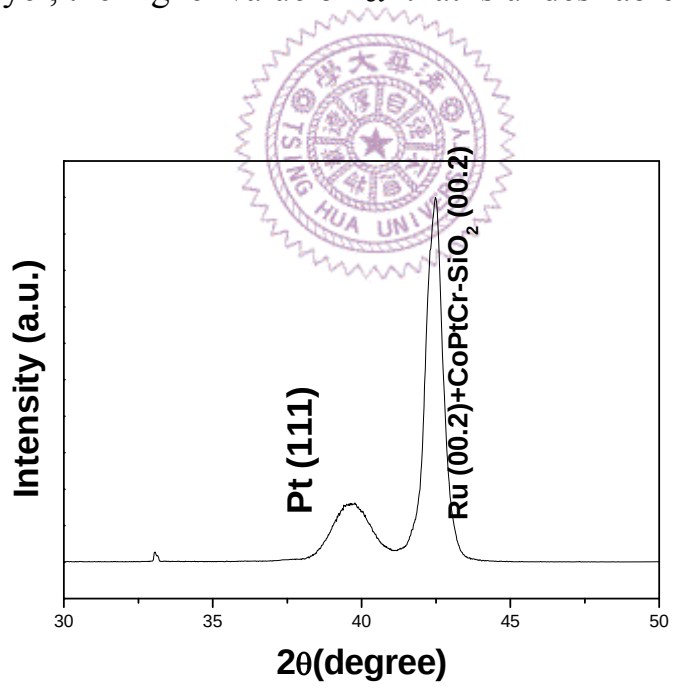

Figure 4- 1 XRD patterns of Ta/CoPtCr-SiO_2/Ru/Pt/Ta/Sub.

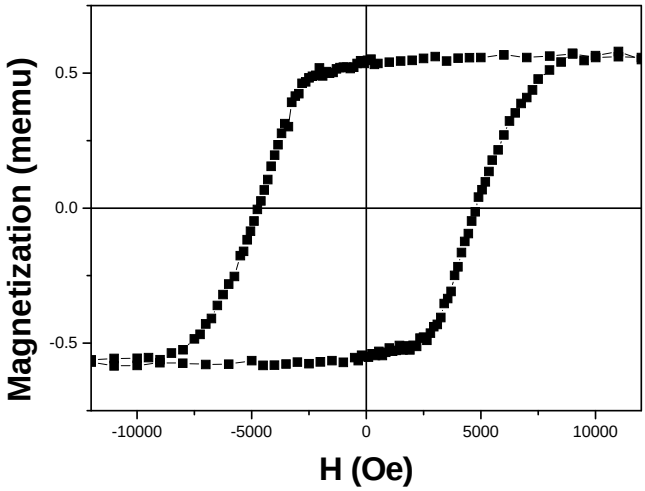

Figure 4- 2 Hysteresis loop of the full-stack perpendicular recording media

The cross-sectional TEM image and plane view TEM image are shown in Figure 4- 3, and the grain size distribution is calculated, as shown in Figure 4- 4. The average grain size is around 8.72nm.

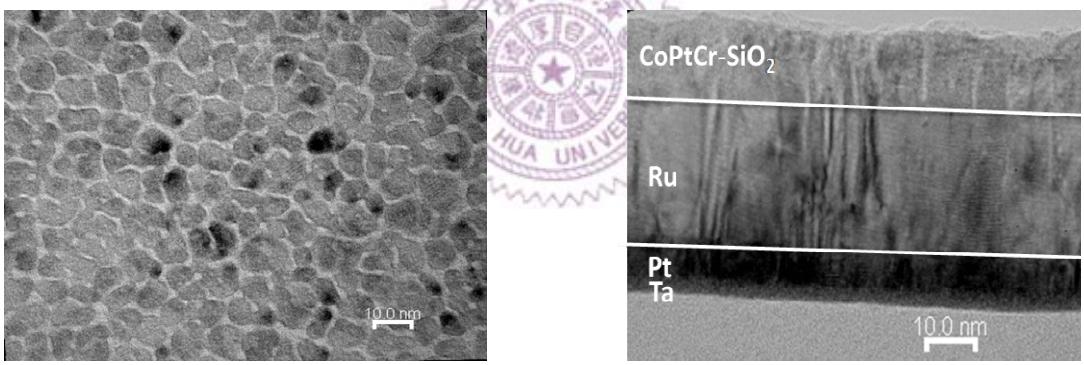

Figure 4- 3 (a) Plane view TEM image and (b) cross-section TEM image of the full-stacked CoPtCr-SiO_2 perpendicular recording media

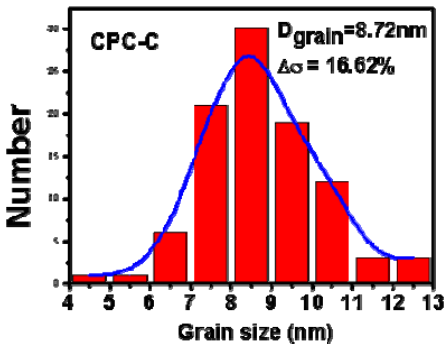

Figure 4- 4 Grain size distribution of CoPtCr-SiO_2layer

The thickness of the intermediate layer in the current full-stacked perpendicular recording media is 30nm that is too thick for the media with the recording density surpassing 1Tbit/in^2. It is necessary to further improve the intermediate layer.

4.2 Improvement on the Intermediate Layers

There are two main functions for the intermediate layers. One is the exchange breaking layers, which decouple the exchange coupling between the soft underlayer and the recording layer. Another is to provide the proper epitaxial condition for the recording layer. Nowadays, the most suitable for the intermediate layer in the recording medium with the CoPtCr-SiO_2 recording layer is Ru [45]. Ru can provide good epitaxial condition because of the small lattice mismatch between CoPtCr-SiO_2 and Ru. Furthermore, the adequate surface roughness of Ru layer can improve the segregation of Cr and SiO_2 in the grain boundary of the recording layer that will decrease the exchange coupling between the grains in the recording layer so as to increase the SNR ratio. However, due to the writability of the recording media and the high cost of Ru, it is necessary to decrease the thickness of Ru layer or to find an alternative material. The main purpose of this thesis is to reduce the thickness of Ru layer and to find an alternative material for Ru.

4.2.1 Ta/Ru Intermediate Layers

In T. Keitoku's study [46], he indicated that Ta layer deposited under Ru layer can promote Ru (00.2) texture because of the less difference of the

surface energy between Ta and Ru. In 2006, W. K. Shen also pointed out that due to epitaxial growth of Ru (00.2) on Ta (110) with a smooth surface, the Ta layer can promote (00.2) texture of the Ru layer [47]. In this section, the effects of Ta layer on Ru layer will be discussed.

4.2.1.1 Effect of Deposition Power of Ta Layer

The relationship between the deposition power of Ta layer and the Ru (00.2) texture was investigated. The films with the layer structure: Ta 3nm/Ru 15nm/Ta 3nm, were prepared. The bottom Ta layers were deposited by different deposition powers. Figure 4- 5 shows the θ-2θ XRD scans. The Ru hcp(0002) peak positions do not shift apparently. Figure 4- 6 shows the c-axis distribution, $\triangle\theta_{50}$, of the Ru layer, and Figure 4- 7 shows the c-axis distribution $\triangle\theta_{50}$ of the Ru layer as a function of the deposition power of Ta layer. The c-axis distributions $\triangle\theta_{50}$ of the Ru layer deposited on the different Ta layers with different deposition power were almost the same. The relationship between the deposition power of the Ta layer and the Ru hcp (00.2) texture was unapparent in this case.

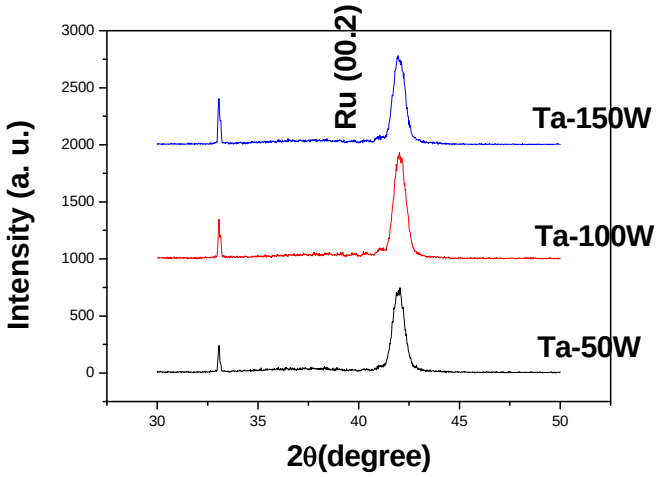

Figure 4- 5 XRD Patterns of Ta/Ru/Ta/Sub. with different deposition power of the bottom Ta layer

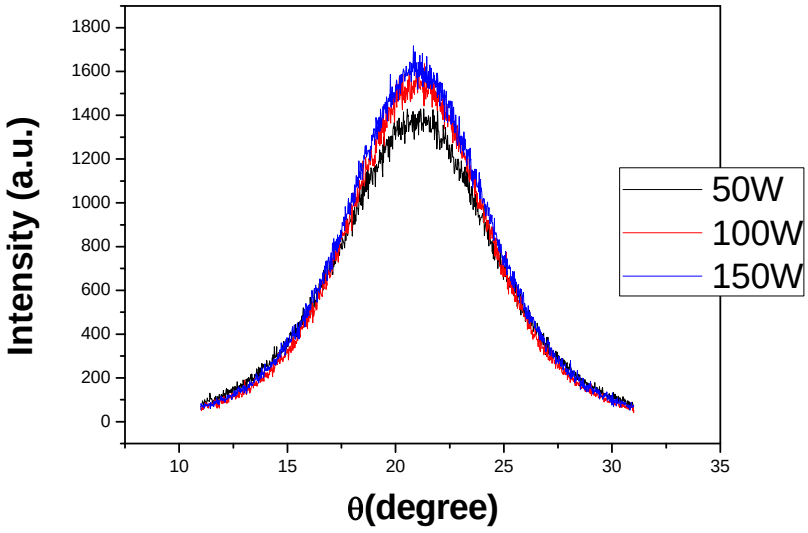

Figure 4- 6 Rocking curves of Ru (00.2) peaks of samples with Ta layers deposited by different powers.

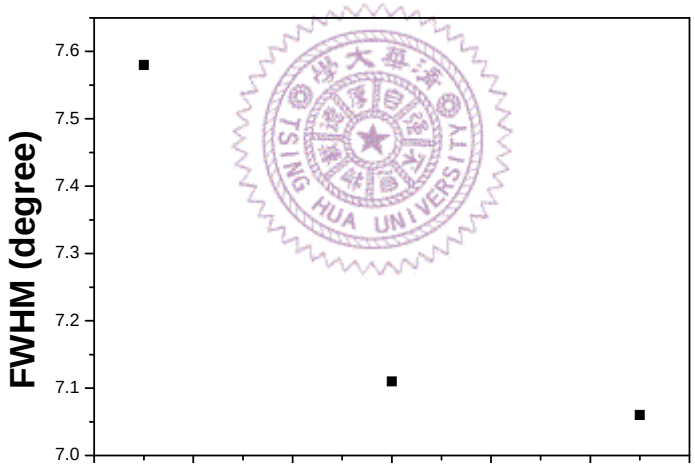

Figure 4- 7 The FWHM of Ru hcp(0002) peaks as a function of different deposition power of Ta layer

4.2.1.2 Effect of Ta Layer Thickness

In 2006, W. K. Shen indicated that the Ta (110) texture with a smooth surface promoted the Ru (00.2) texture [47]. The thicker film thickness will help the form of texture, so the relationship between the film thickness and the Ru (00.2) texture is discussed here. Figure 4- 8 shows the θ-2θ

XRD scans of the films with different Ta layer thickness. The Ru hcp(00.2) peak position did not shift apparently. Rocking curves of the Ru layer are shown in Figure 4- 9, and the relationship between the Ta layer thickness and the c-axis distribution $\triangle\theta_{50}$ of the Ru layer is shown in Figure 4- 10. When the Ta layer thickness increased from 2.5nm to 5nm, the c-axis distribution $\triangle\theta_{50}$ of the Ru layer dropped from 7.14^0 to 5.66^0. Further increased the Ta layer thickness did not influence $\triangle\theta_{50}$ of the Ru layer a lot. It seems that the 5nm thickness of Ta layer is enough to promote the Ru (00.2) texture. Those peaks near the Ru (00.2) peak with weak intensity need to be further identified.

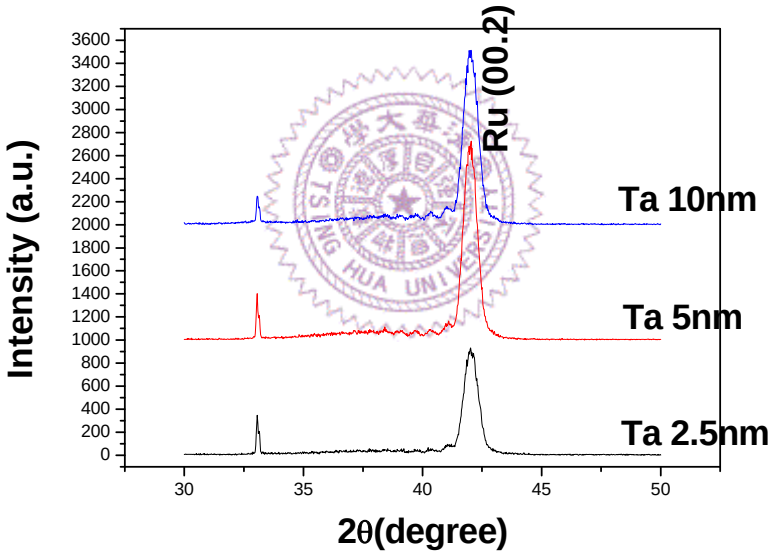

Figure 4- 8 XRD patterns of Ta/Ru/Ta/Sub. with different Ta layer thickness

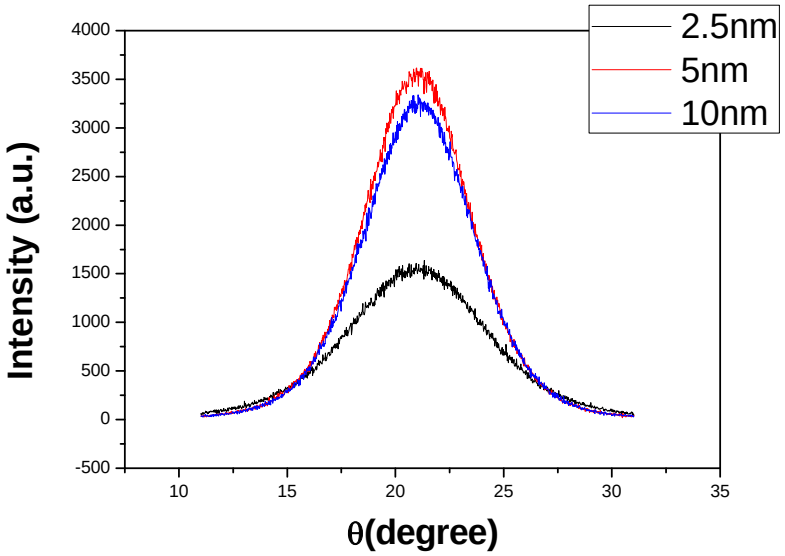

Figure 4- 9 Rocking curves of the Ru hcp(00.2) texture of samples with different Ta layer thickness

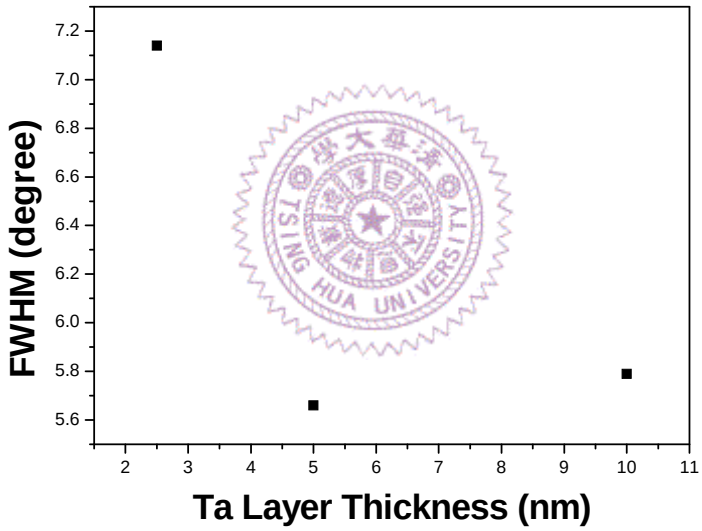

Figure 4- 10 The FWHM of Ru (00.2) peaks plotted as a function of Ta layer thickness (nm)

In conclusion, the Ta layer with proper layer thickness will promote Ru (00.2) texture well.

4.2.2 Effect of NiW and Pt

The film with a face-centered-cubic (fcc) [111] orientation out of plane can promote a Ru hcp [00.2] perpendicular orientation. NiW is one of the suitable materials. From the phase diagram of NiW shown in Figure 4- 11, Ni with 8 to 12 at% of W can eliminate the ferromagnetic property of Ni and the alloy is still a fcc structure. The distance between the nearst atoms on the close-packed (111) plane is 0.262nm, and the lattice mismatch between NiW and Ru is only 3.1%. So we can expect that NiW can provide a good epitaxial condition for the growth of Ru. Figure 4- 12(a) shows the θ-2θ scan results of the films with the NiW intermediate layer. The layer structure was: Ta 3nm/NiW 7nm/Ru 30nm/CoPtCr-SiO_2 17.5nm/Ta 3nm. All the peak positions of Ru (00.2) ,NiW (111) and Co(00.2) are overlapped. The Pt film with a fcc orientation can be the candidate. The θ-2θ XRD scan results of the film with Pt intermediate layer is shown in figure. The film structure was: Ta 3nm/Pt 7nm/Ru 30nm/CoPtCr-SiO_2 17.5nm/Ta 3nm. Figure 4- 12(b) shows the hysteresis loops of the films with the NiW intermediate layer and the Pt intermediate layer, respectively, and Table 4. 1 shows the coercivity, the nucleation field and the squareness of the hysteresis loops. The texture of the recording layer deposited on the NiW intermediate layer is better because of the better nucleation field and the squareness of the hysteresis loop. However, the coercivity of the film with the NiW intermediate layer is lower. It seems that the coercivity isn't directly proportional to the texture of the recording layer.

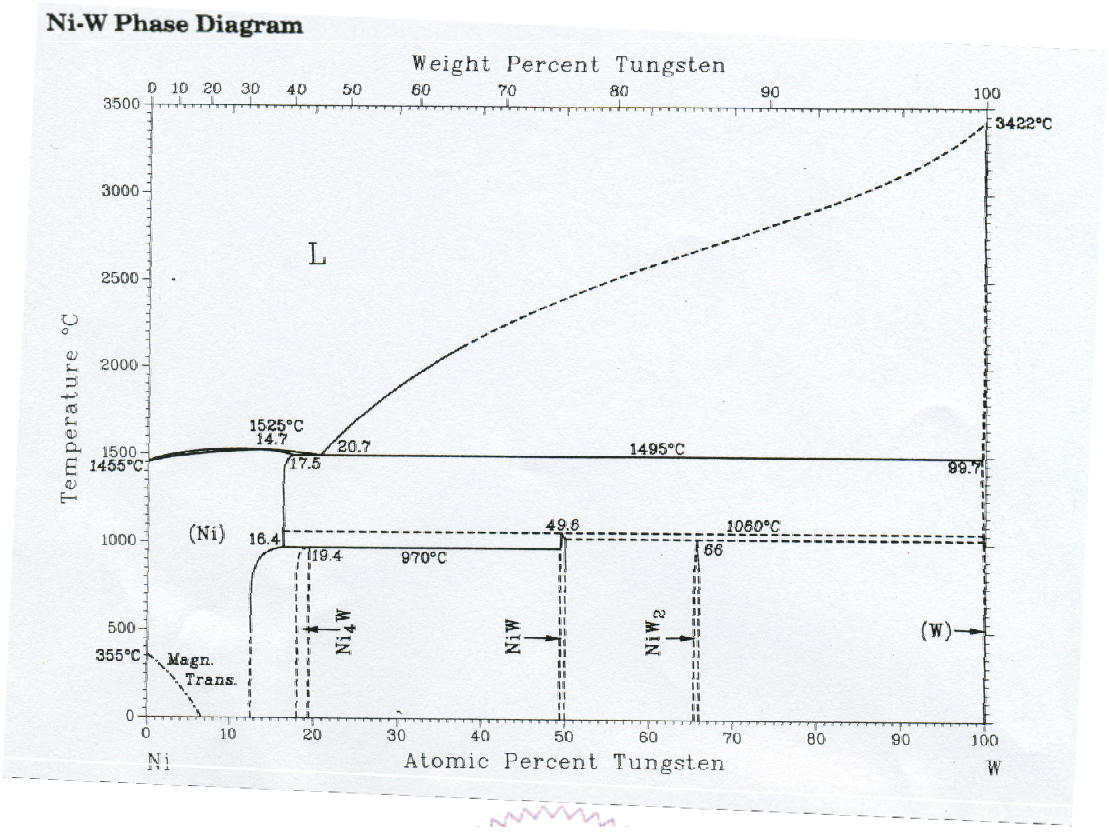

Figure 4- 11 The phase diagram of NiW

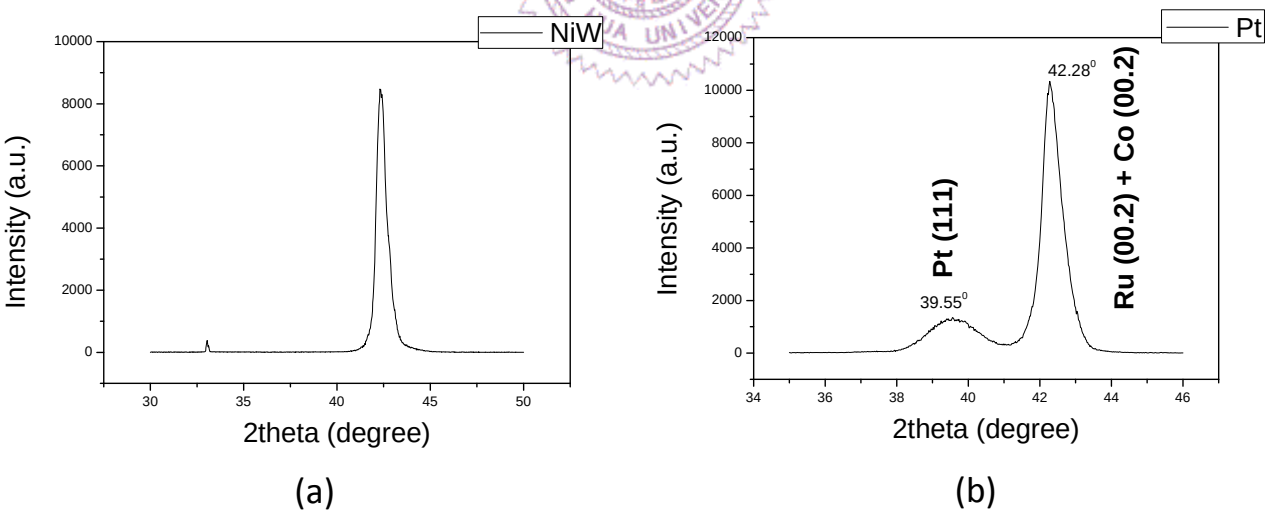

Figure 4- 12 The θ-2θ scan results of the PMR films with (a) NiW intermediate layer and (b) Pt intermediate layer

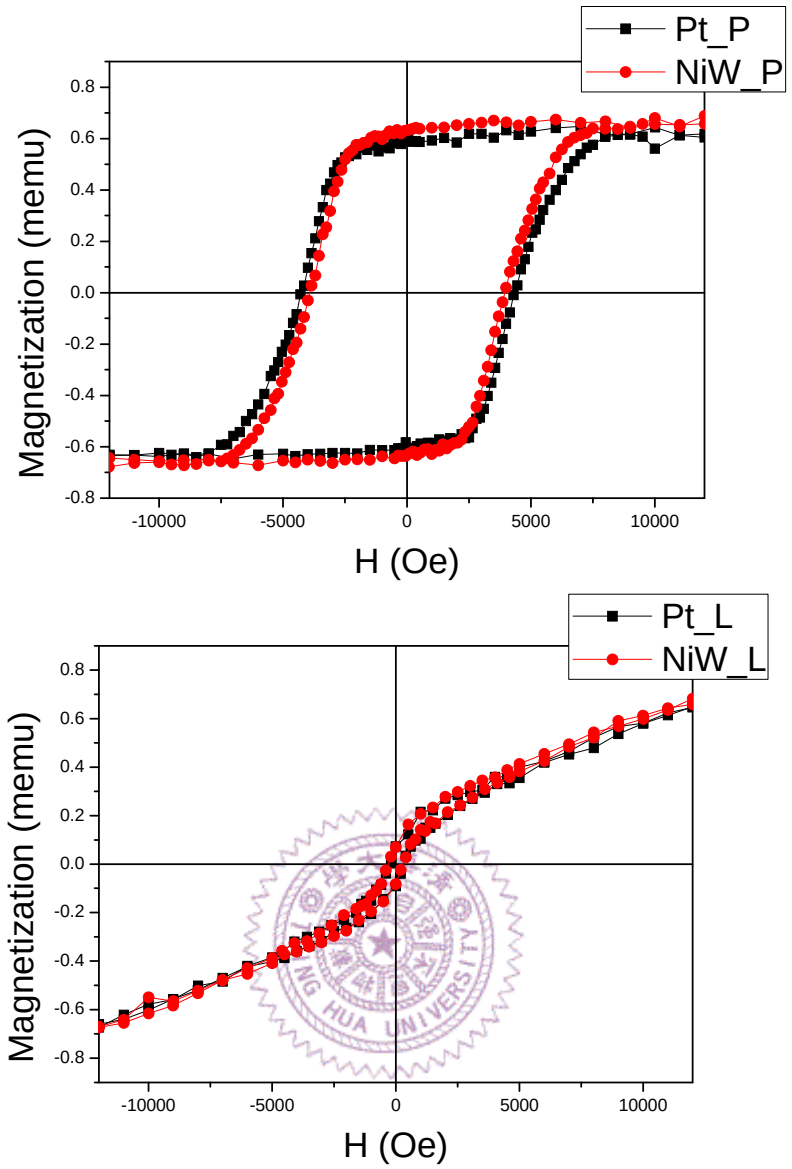

Figure 4- 13 The hysteresis loops of the films with Pt intermediate layer and NiW intermediate layer, respectively

Table 4. 1 The coercivity, nucleation field and squareness of the hysteresis loops of the PMR films with the Pt intermediate layer and the NiW intermediate layer, respecitvely

	Pt	NiW
Hc (Oe)	4299	3934
Hn (Oe)	-400	-862
S	0.94	0.95

4.2.2 Dual Ru Intermediate Layers

Recently, the media with the dual-Ru layer was widely used [49]. In the dual-Ru layer structure, the bottom Ru layer was deposited in a high mobility condition that can help to achieve a good crystalline texture, and the upper Ru layer was deposited in a low mobility condition that can promote the formation of a columnar structure. According to the Thornton diagram as shown in Figure 4- 14[48], the formation of void intergrain boundaries is pronounced at higher deposition pressure. So in the following sections the upper Ru layers were prepared at a high argon pressure. In the first section, the optimized media with the dual-Ru layer structure was investigated.

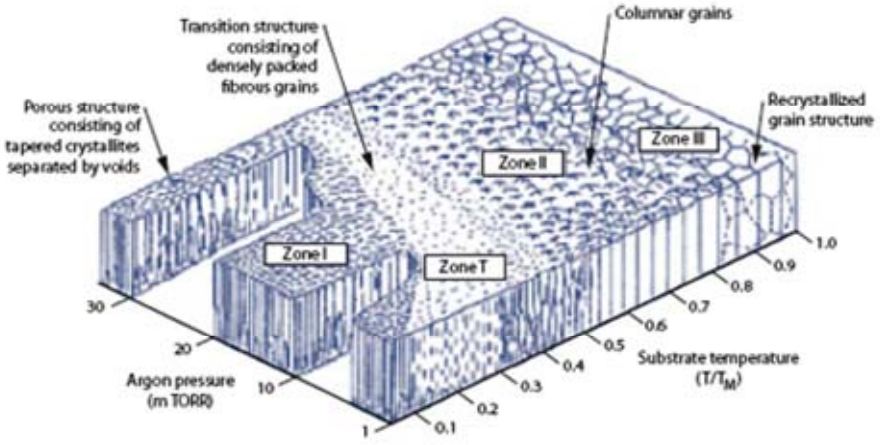

Figure 4- 14 The Thornton Diagram [48]

4.2.2.1 Effect of Deposition Power of the Top Ru Layer

The influence of the deposition power of the top Ru layer on the performance of the magnetic film is discussed here. Due to the need of the low mobility condition of the top Ru layer, we decreased the deposition

power of the top Ru layer from 125W to 50W. The layer structure was: Ta 3nm/Pt 7nm/Ru_b 15nm/Ru_t 5nm/CoPtCr-SiO_2 17.5nm/Ta 3nm. The bottom Ru layer was deposited by dc 125W with substrate bias 125V at 3mTorr for the high mobility condition. The top Ru layer was deposited by different dc watts without substrate bias at 50mTorr for the low mobility condition. Figure 4- 15 shows the θ-2θ XRD scans of the films with different top Ru layers deposited by using different deposition power. The Ru hcp(00.2) peak positions and Co hcp(00.2) positions did not shift apparently. Rocking curves are shown in Figure 4- 16, and the relationships between the deposition powers and the c-axis distribution of Ru and Co are show in Figure 4- 17. Increasing the deposition power of the top Ru layer can promote the mobility of Ru atoms that will help to promote the Ru (00.2) texture. However, the help is unapparent here.

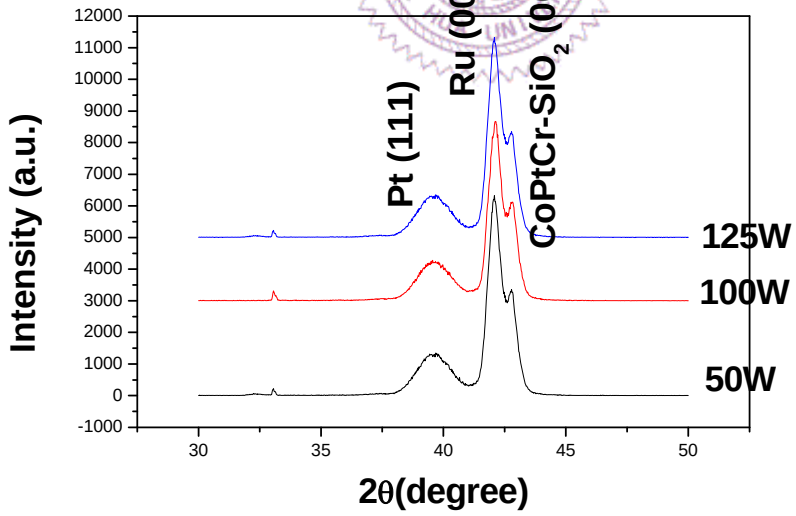

Figure 4- 15 XRD patterns of the films with different top Ru layers deposited by different powers

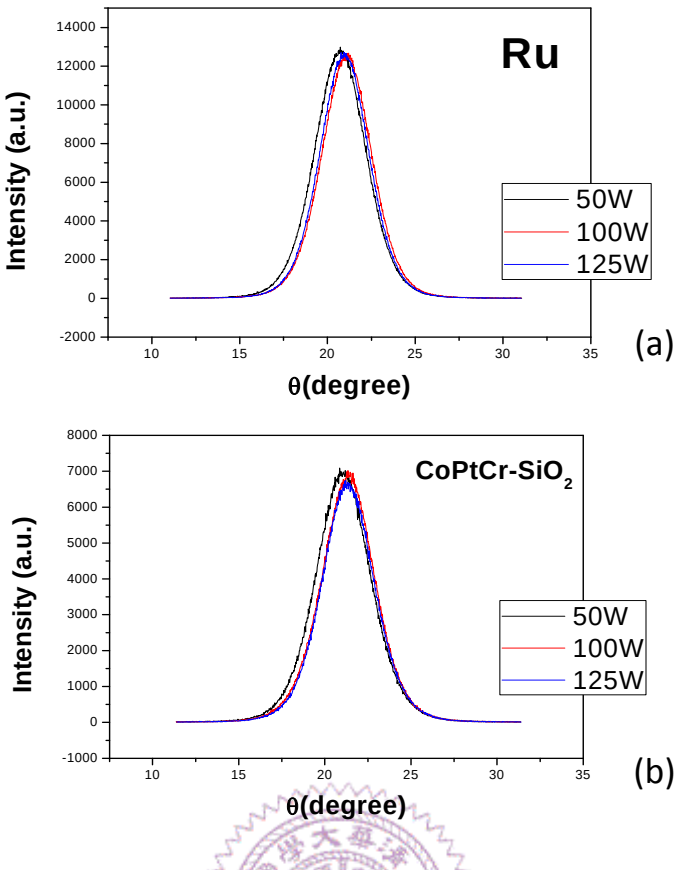

Figure 4- 16 Rocking Curves of (a) the Ru (00.2) peaks and (b) the Co (00.2) peaks of the films with different top Ru layers deposited by different powers

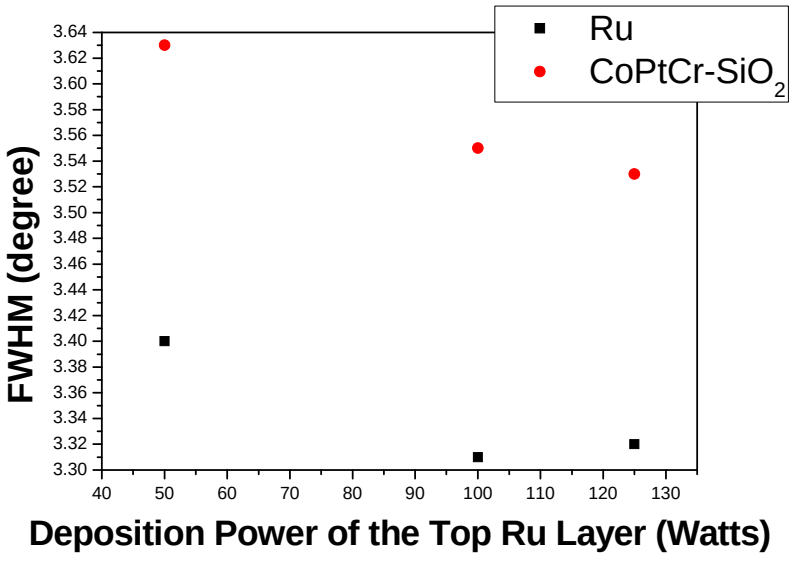

Figure 4- 17 $\triangle\theta_{50}$ of Ru and CoPtCr-SiO_2 (00.2) peaks as a function of the deposition power of the top Ru layer

The hysteresis loops were shown in Figure 4- 18, and the relationship between the deposition power of the top Ru layer and the coercivity was shown in Figure 4- 19. It was found that the coercivity increased with decreasing the deposition power of the top Ru layer. However, the $\triangle\theta_{50}$ of CoPtCr-SiO_2 (00.2) peaks increased with decreasing the deposition power of the top Ru layer, that means the hcp(00.2) texture of the CoPtCr-SiO_2 layer became worse. The most possible mechanism of the increased coercivity is the increased surface roughness of the top Ru layer with decreasing the deposition power. The α value decreased with decreasing the deposition power of the top Ru layer, as shown in Figure 4-20. The results indicated that the exchange coupling between grains decreased with decreasing the deposition power and the coercivity of the films increased. Decreasing the deposition power provided a low mobility condition when deposited the top Ru layer so as to roughen the surface of the top Ru layer. A proper rough surface of the top Ru layer can help the segregation of SiO_2 and Cr in the grain boundary of CoPtCr-SiO_2 recording layer, and it reduces the exchange coupling between the grains in the recording layer. The coercivity increases with decreasing the exchange coupling between grains in the recording layer.

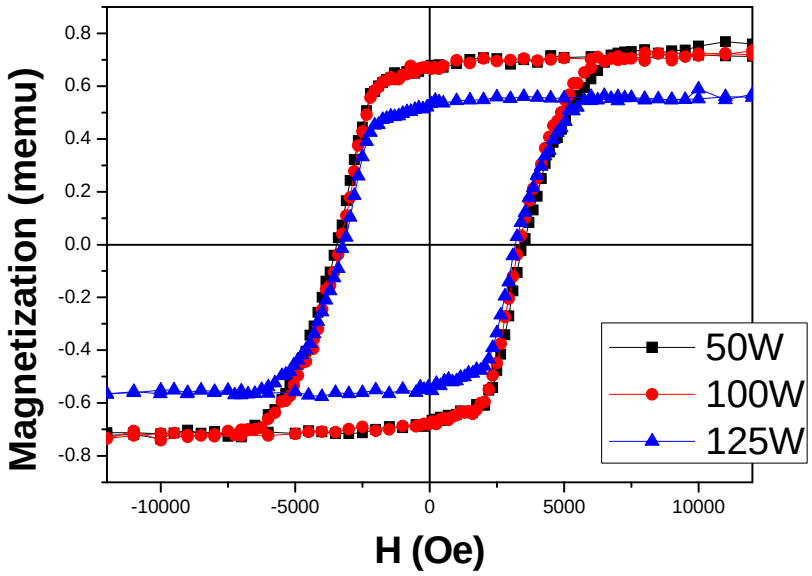

Figure 4- 18 Hysteresis loops of CoPtCr-SiO_2 films with Ru layers deposited by different deposition power

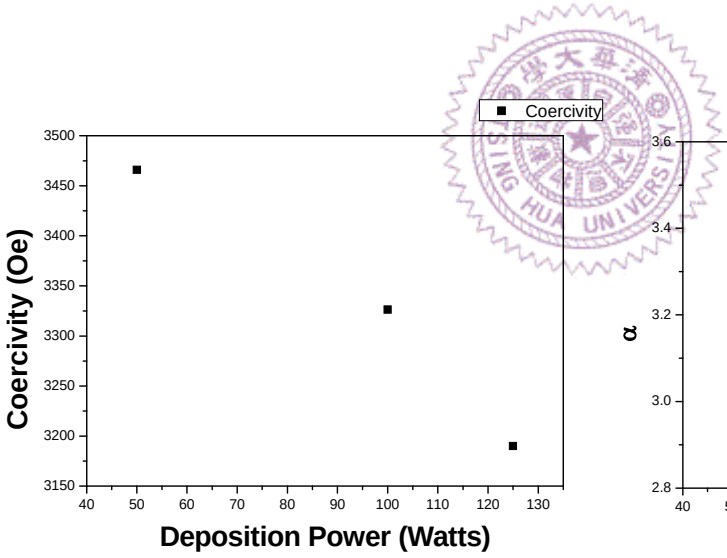

Figure 4- 19 Coercivity of CoPtCr-SiO_2 media as a function of the deposition power of the top Ru layer

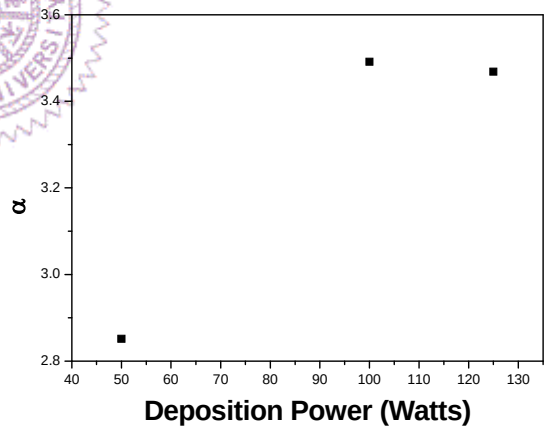

Figure 4- 20 α value as a function of the deposition power of the top Ru layer

4.2.2.2 Effect of the Bottom Ru Layer Thickness

The effects of the bottom Ru layer are investigated in this section. The films with different bottom Ru layer thickness are prepared. The film structure is: SiO_2 substrate/Ta 3nm/Pt 7nm/Ru_b xnm/Ru_t 5nm/ CoPtCr-SiO_2 17.5nm/Ta 3nm. The top Ru layer was deposited by dc 50W without substrate bias at 50mTorr for the low mobility condition, and the top Ru layer was deposited by dc 125W with substrate bias 125V at 3mTorr for the high mobility condition. The θ-2θ XRD scans of the films with different bottom Ru layer thickness are shown in Figure 4- 21. It can be seen that the intensity of Ru hcp(00.2) peak increases apparently with increasing the thickness of the bottom Ru layer. Figure 4- 22 shows the $\triangle\theta_{50}$ of Ru hcp(00.2) peaks and $\triangle\theta_{50}$ of CoPtCr-SiO_2 hcp(00.2) peaks as a function of the bottom Ru layer thickness. Both the $\triangle\theta_{50}$ of Ru and the $\triangle\theta_{50}$ CoPtCr-SiO2 decrease gradually with increasing the bottom Ru layer thickness. The increasing of the bottom Ru layer thickness promoted Ru hcp(00.2) texture and Co hcp(00.2) texture obviously. However, the media with thick intermediate layer have lower writability that is undesirable. A proper thickness of Ru layer equal to 15nm is chosen.

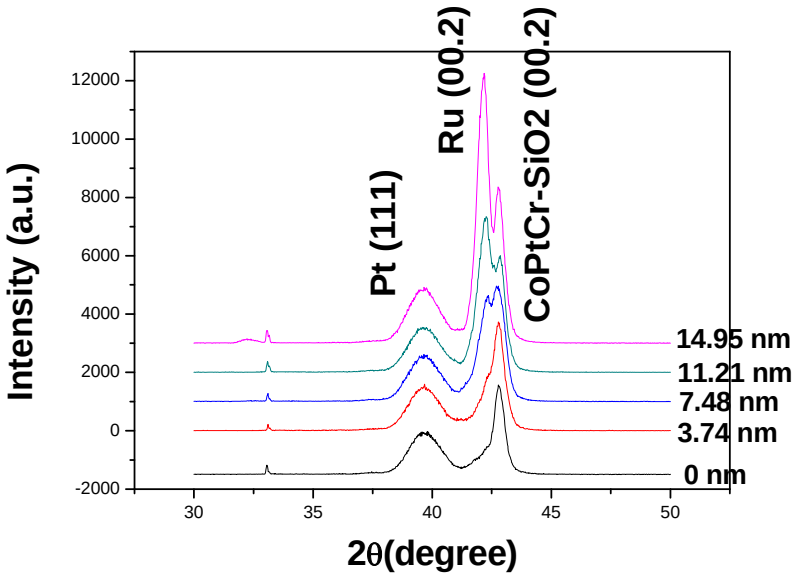

Figure 4- 21 XRD patterns of CoPtCr-SiO_2 films with different bottom Ru layer thickness

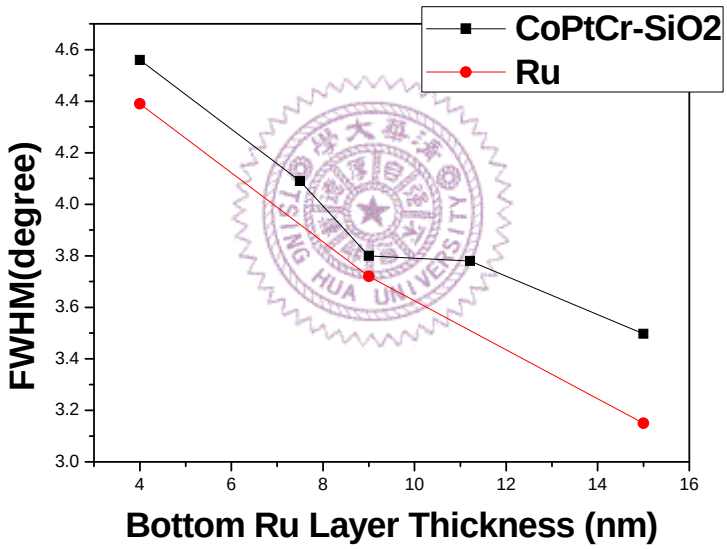

Figure 4- 22 Rocking Curves of Ru and Co (0002) peaks as a function of the bottom Ru layer thickness

The hysteresis loops are shown in Figure 4- 23, and the relation between the coercivity and the bottom Ru layer thickness are shown in Figure 4- 24. The coercivity increases with increasing the bottom Ru layer thickness. It can be concluded that increasing the bottom Ru layer thickness can promote Ru hcp(00.2) texture. The well-alignment c-axis of Ru layer can

induce highly oriented CoPtCr-SiO_2 recording layer, and the coercivity of the CoPtCr-SiO_2 recording media can be enhanced.

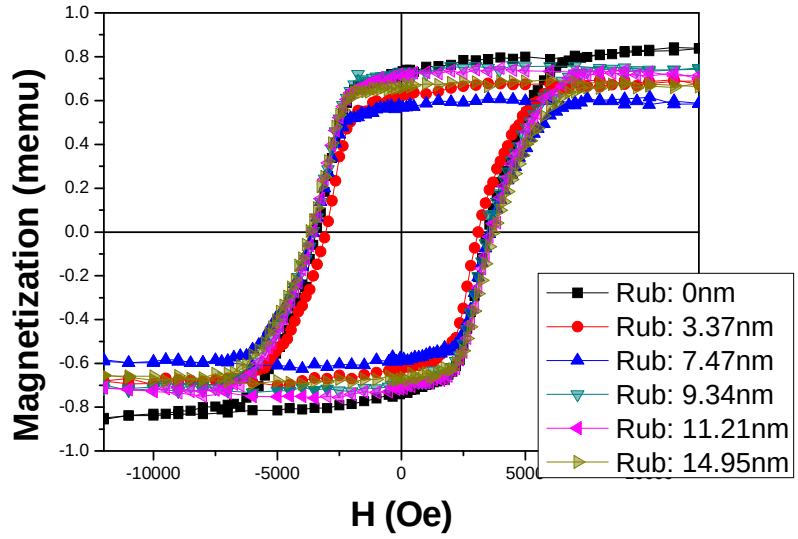

Figure 4- 23 Hysteresis loops of the films with different bottom Ru layer thickness

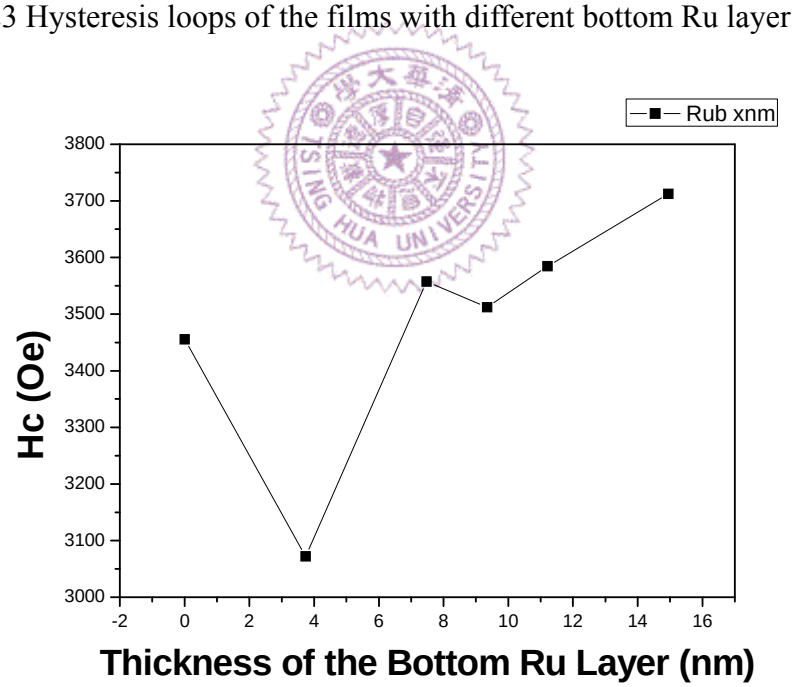

Figure 4- 24 Hc as a function of the bottom Ru layer thickness

4.2.2.3 Effect of the Thickness Ratio of the Bottom Ru Layer Thickness to the Top Ru Layer Thickness

In this section, the films with different thickness ratio of the bottom Ru layer to the top Ru layer are investigated. The film structure is: Ta 3nm/Pt 7nm/Ru_b xnm/Ru_t ynm/CoPtCr-SiO_2 17.5nm/Ta 3nm. The bottom Ru layer was deposited at dc125W with substrate bias 125V at 3mTorr for the high mobility condition and the top Ru layer was deposited at dc50W without substrate bias at 50mTorr for the low mobility condition. The total thickness of the bottom Ru layer and the top Ru layer is fixed at 20nm. The θ-2θ XRD scans are shown in Figure 4- 25. When the thickness of the bottom Ru layer thickness increases, the Ru hcp(00.2) peak intensity increases apparently. Figure 4- 26 shows the rocking curves of CoPtCr-SiO_2 hcp(00.2) peaks, and $\triangle\theta_{50}$ of CoPtCr-SiO_2 hcp(00.2) peaks as a function of the bottom Ru layer thickness is shown in Figure 4- 27. When the ratio of the bottom Ru layer thickness to the top Ru layer thickness decreases, $\triangle\theta_{50}$ of CoPtCr-SiO_2 hcp(00.2) peaks decrease obviously that means the less c-axis dispersion of CoPtCr-SiO_2 recording layer.

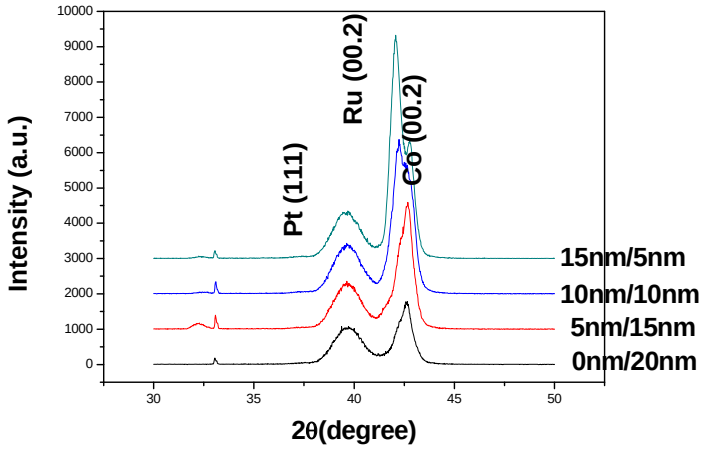

Figure 4- 25 XRD patterns of the films with different thickness ratio of the bottom Ru layer thickness to the top Ru layer thickness

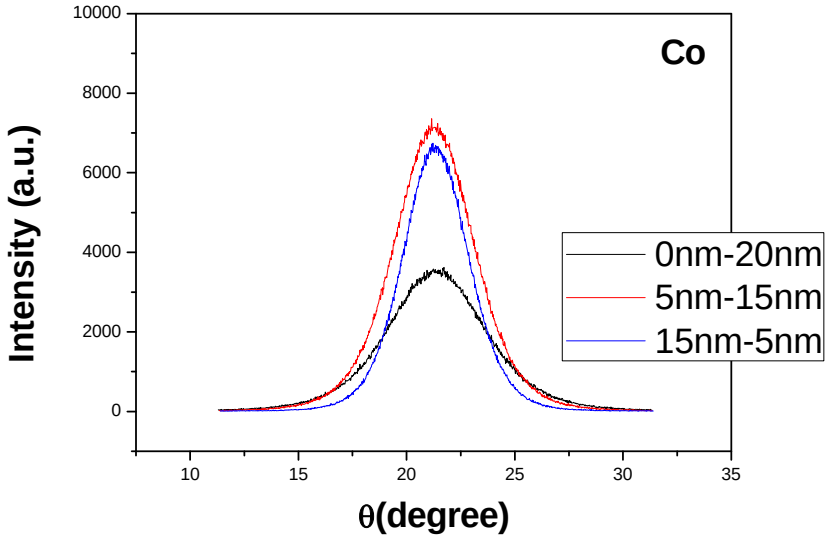

Figure 4- 26 Rocking curves of Co hcp(00.2) peaks of films with different thickness ration of the bottom Ru layer to the top Ru layer

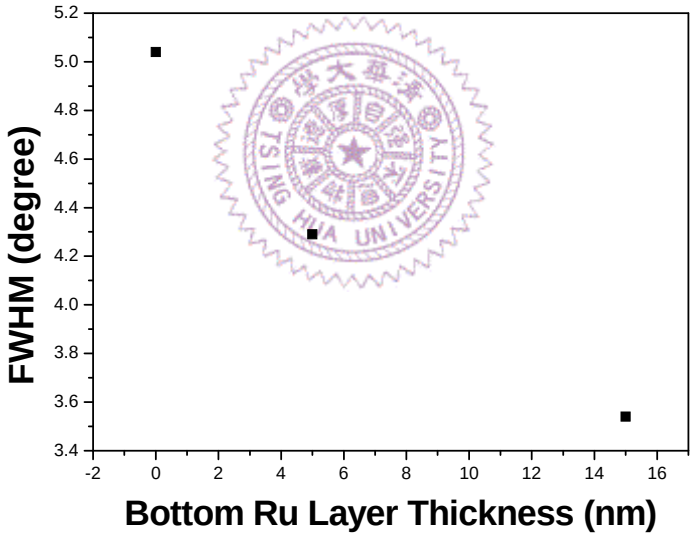

Figure 4- 27 $\triangle\theta_{50}$ of CoPtCr-SiO_2 hcp(00.2) peaks as a function of the bottom Ru layer thickness

The hysteresis loops are shown in Figure 4- 28, and the relation between the coercivity and the bottom Ru layer thickness is shown in Figure 4- 30. The coercivity decreases at first when the bottom Ru layer thickness increases from 0nm to 5nm and it increases as increasing the bottom Ru layer thickness from 5nm to 15nm. The α values are calculated and the

results as a function of the bottom Ru layer thickness is shown in Figure 4-29. The α value of the film without the bottom Ru layer is lowest that means the exchange coupling between the grains in the recording layer is weakest. The top Ru layer provides proper surface roughness to promote the segregation of SiO_2 and Cr in the grain boundary of the CoPtCr-SiO_2 recording layer so as to decrease the exchange coupling between the grains in the recording layer, and the coercivity increases. Because the texture of the film without the bottom Ru layer is much worse than the textures of the films with the bottom Ru layer, the coercivity of the film without the bottom Ru layer is not very high. The bottom Ru layer is needed to promote the hcp(00.2) texture of CoPtCr-SiO_2 layer. On the other hand, $\triangle\theta_{50}$ of CoPtCr-SiO_2 hcp(00.2) peaks of the film with bottom Ru layer thickness 15nm is lowest that means the hcp(00.2) texture of the recoding layer is better than others. However, the coercivity is not high because of the relative high α value. It seems that the bottom Ru layer with layer thickness 15nm can well promote hcp(00.2) texture of CoPtCr-SiO_2 recording layer, but the surface roughness of the top Ru layer with 5nm layer thickness is not good enough. Ru layer with higher surface roughness at lower layer thickness is needed to further investigate.

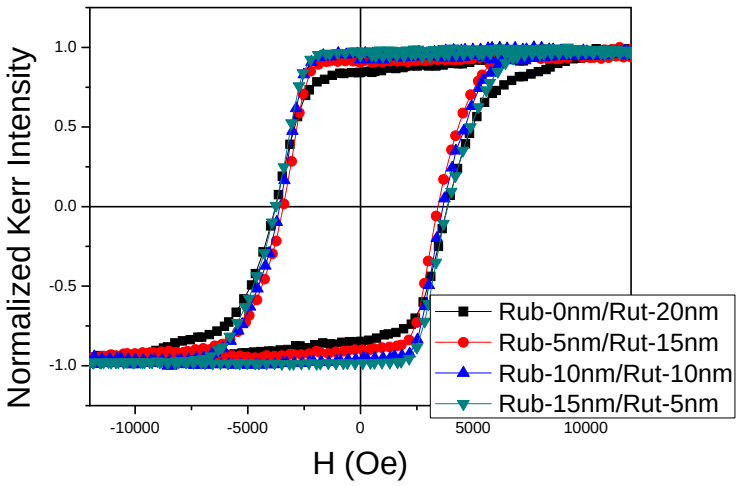

Figure 4- 28 Hysteresis loops of the films with different thickness ratio of the bottom Ru layer thickness to the top Ru layer thickness

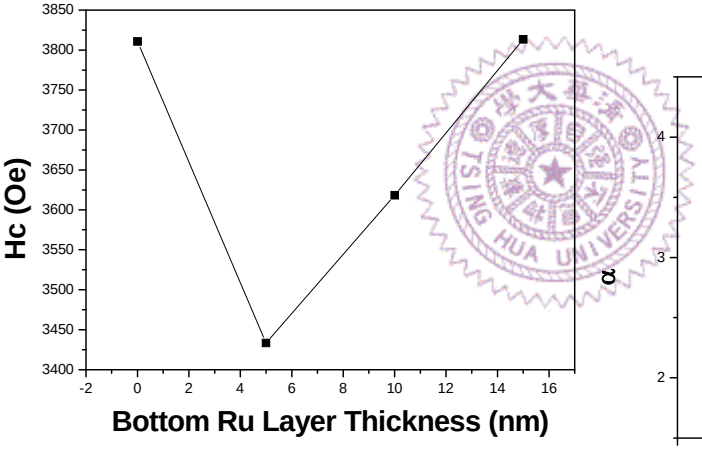

Figure 4- 30 Hc as a function of the bottom Ru layer thickness

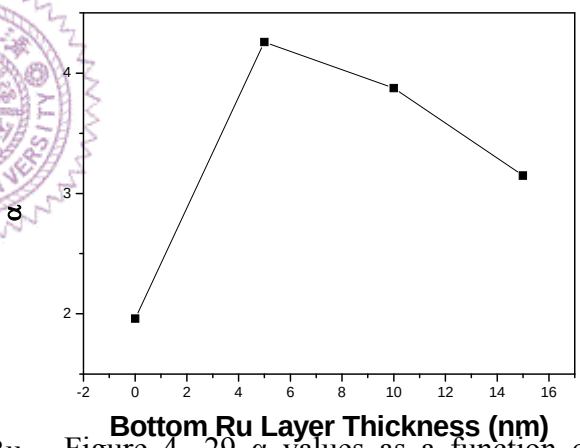

Figure 4- 29 α values as a function of the bottom Ru layer thickness

4.2.3 MnRu Intermediate Layer

Invesitgation of MnRu to be one of the possible substitutes for Ru is shown here. Figure 4- 31 shows the phase diagram of MnRu. MnRu alloy with concentration of Ru between 31 at% to 37 at% is the disordered γ-phase and the crystal structure of MnRu is faced center cubic (FCC), as shown in Figure 4- 32[50]. The lattice constant of MnRu alloy is about 0.377nm and it slightly increases with increasing Ru concentration. The distance between the nearest atoms in the closed packed plane ((111) plane) is about 0.267nm, and the lattice mismatch between MnRu and the CoPtCr-SiO2 recording layer is 3.1%, that is quite good for the hetero-epitaxial growth.

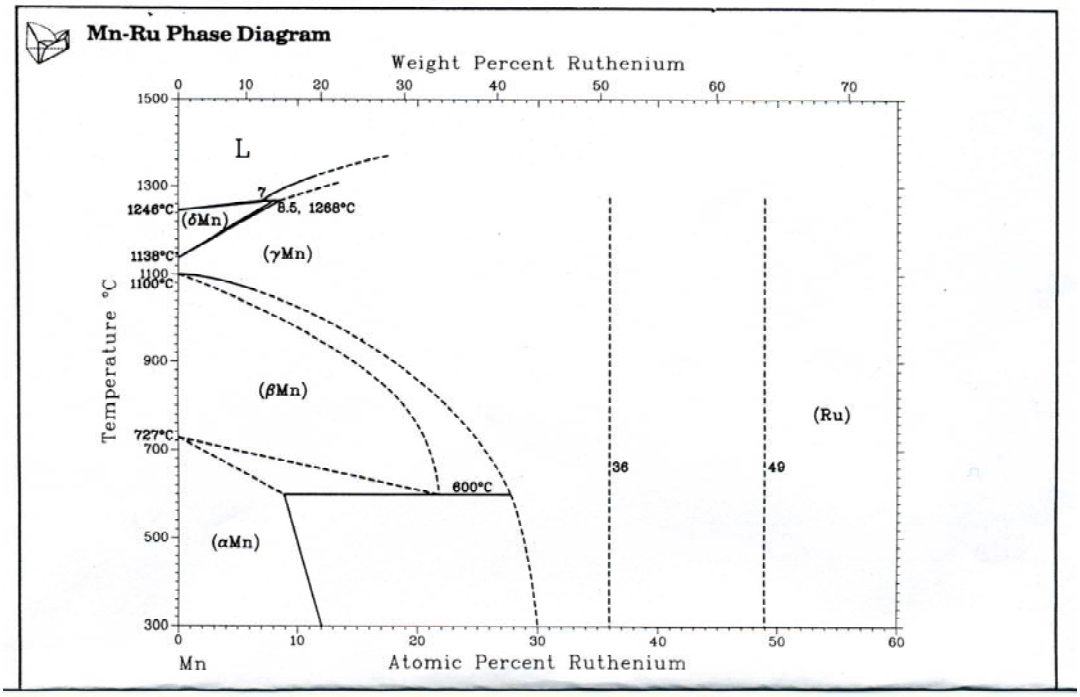

Figure 4- 31 The MnRu phase diagram

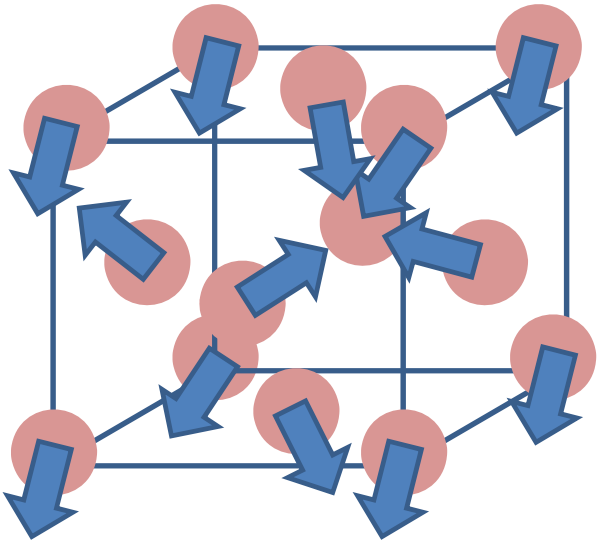

Figure 4- 32 The crystal structure of MnRu. The arrows mean the disorder magnetization of Mn.

IThe PMR films with MnRu intermediate layer were prepared. The layer structure was: Ta 3nm/Pt 7nm/MnRu 20nm/CoPtCr-SiO_2 17.5nm/Ta 3nm. The MnRu layers with different Ru at% were prepared by co-sputtering method. The Mn deposition power was fixed at dc100W and the Ru deposition power was changed from 40W to 100W. The θ -2θ XRD scans are shown in Figure 4- 33. The peak position of the MnRu layer first shifted to the lower angle with increasing the Ru depositon power and shifted back with further increasing the Ru deposition power. The reason may as follows: the layer structure of the MnRu layer deposited by dc100W of Mn and dc40W of Ru was face centered cubic (FCC) and further increasing the concentration of Ru increased the lattice constant of the MnRu layer so as to shift the peak position to the left. With higher concentration of Ru in the MnRu layer, the texture of the MnRu layer transferred from FCC to HCP structure and further increasing the concentration of Ru shifted the peak position to the right.

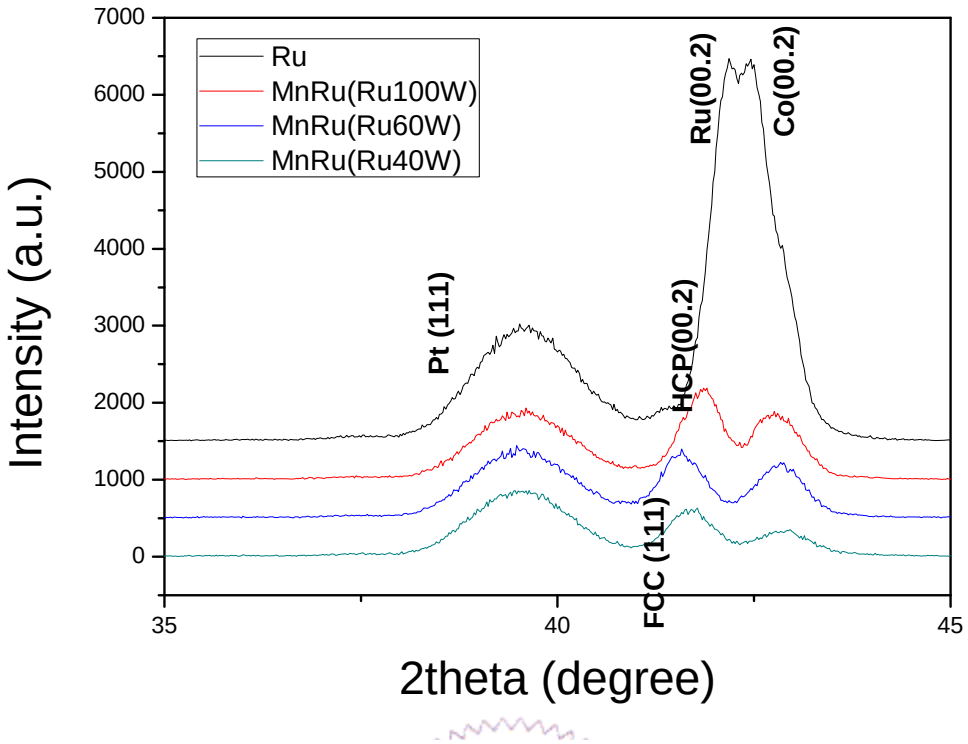

Figure 4- 33 The θ-2θ XRD scans of the films with MnRu intermediate layer and with pure Ru layer, respectively

The hysteresis loops of the films with different MnRu layers and with Ru layer only were shown in Figure 4- 34, and the coercivity and the squareness of the films were shown in the Table 4. 2. It can be seen that the squareness increased with increasing the contents of Ru in the MnRu layer and the coercivity of the films with the MnRu layer deposited by dc100W of Mn and by dc100W of Ru equaled to 4932 Oe that was highest. There were two main reasons that influenced the squareness of the hysteresis loop: the texture of the recording layer and the grain size distribution in the recording layer. When increased the Ru contents in the MnRu layer, it might help the epitaxial growth of the recording layer or it helped the SiO_2 segregation at the grain boundary of the recording layer that shrinks the grain size distribution. From the XRD results and the magnetic

properties, we could not make any conclusion yet. Further investigations were needed.

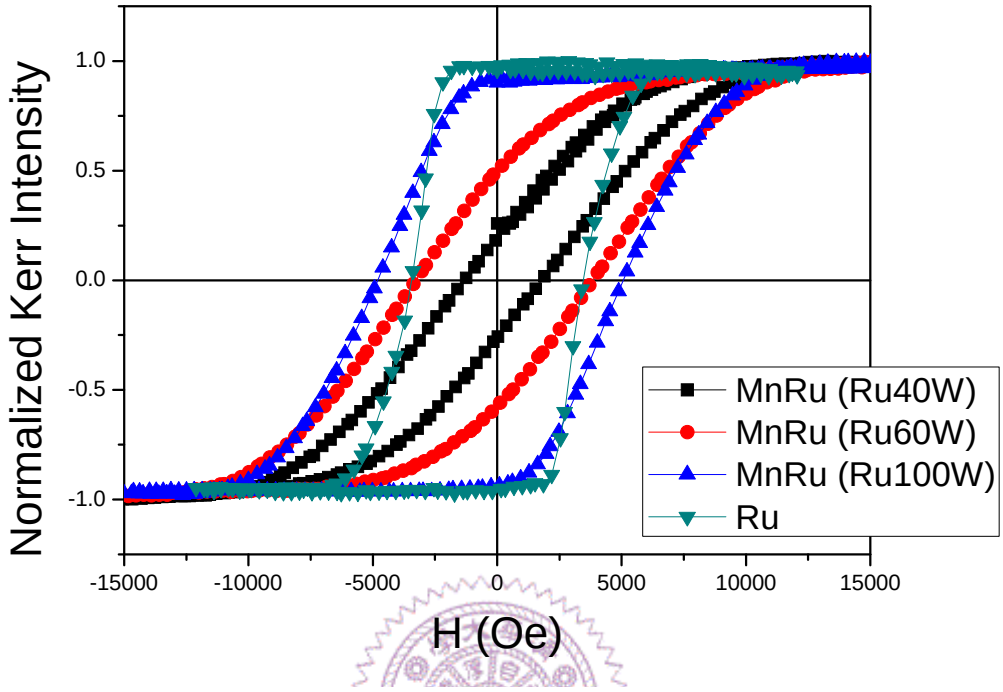

Figure 4- 34 The hysteresis loops of the films with different MnRu layers and with Ru layer only, respectively

Table 4. 2 The coercivity and squareness of the films with different intermediate layers

	Ru	MnRu (Ru100W)	MnRu (Ru60W)	MnRu (Ru40W)
Hc (Oe)	**3452**	**4932**	**3553**	**1561**
S	**1**	**0.97**	**0.55**	**0.23**

It can be concluded that the media with MnRu intermediate layer with hcp structure exists better magnetic properties than the media with MnRu intermediate layer with fcc structure. Further analyzing on the microstructure of the intermediate layer is needed.

Chapter 5 Summary

1. Increasing the deposition power of Ta underlayer can further promote Ru hcp(00.2) texture slightly. It may cause from the higher mobility of Ta atoms that can produce the smooth surface of Ta layer when increase the deposition power of Ta layer. A proper Ta layer thickness can effectively improve Ru hcp(00.2) texture.
2. The coercivity of CoPtCr-SiO_2 perpendicular recording media decreased with increasing the deposition power of the top Ru layer.
3. Increasing the bottom Ru layer thickness can promote Ru hcp(00.2) texture further so as to improve CoPtCr-SiO_2 hcp(00.2) texture and enhance the coercivity.
4. The appropriate thickness ratio of the bottom Ru layer thickness to the top Ru layer thickness can provide the good epitaxial growth condition for CoPtCr-SiO_2 hcp(00.2) texture and the adequate surface roughness that can further promote the coercivity.
5. A new material MnRu is proposed to be the alternative material for Ru. The magnetic performance of the perpendicular recording media with the MnRu layer with hcp phase (Ru rich) is better than the media with the MnRu intermediate layer with fcc phase. Further investigating the texture of the MnRu intermediate layer is needed.

References

[1] S. Iwasaki and K. Takemura, “An analysis for the circular mode magnetization in short wavelength,” IEEE Trans. Magn., 11 (1975) 1173

[2] S. N. Piramanayagam, “Perpendicular recording media for hard disk drives,”J. Appl. Phys. 102, 011301 (2007)

[3] K. Ouchi and N. Honda, “Overview of Latest Work on Perpendicular Recording Media,” IEEE Trans. Magn., 36 (2000) 16

[4] S. H. Charap et al., “Thermal Stability of Recorded Information at High Densities,” IEEE Trans. Magn., 33 (1997) 978

[5] Y. Honda et al., “Effect of soft magnetic underlayer on magnetization microstructure of perpendicular thin film media,” IEEE Trans. Magn., 36 (2000) 2399

[6] J. Ariake et al., “Preparation of double-layered magnetic perpendicular media for fine magnetic structure,” IEEE Trans. Magn., 36 (2000) 2411

[7] M. Zheng et al., “SNR improvement of granular perpendicular media,” IEEE Trans. Magn., 39 (2003) 1919

[8] C. Chang et al., “Measurements and Modeling of Soft Underlayer Materials for Perpendicular Magnetic Recording,” IEEE Trans. Magn., 38 (2002) 1637

[9] C. H. Lai, R. F. Jiang, “Biased FeTaC(N) soft underlayer for perpendicular media,” J. Appl. Phys. 93. 8155 (2003)

[10] M. Miura et al., “Annealing Behavior of Mangetic-anisotropy in CoNBZr Films,” IEEE Trans. Magn., 24 (1988) 2215

[11] M. Futrmoto et al., “Microstructure and Magnetic-Properties of CoCr Thin-Films Formed on Ge Layer,” IEEE Trans. Magn., 21 (1985) 1426

[12] Y. Hirayama, “Ultrathin intermediate template layer for perpendicular recording,” IEEE Trans. Magn., 39 (2003) 2282

[13] Y. Hirayama, “Development of high resolution and low noise single-layered perpendicular recording media for high density recording,” IEEE Trans. Magn., 33 (1997) 996

[14] H. Uwazumi et al., “Recording performance of CoCrPt-(Ta, B)/TiCr perpendicular recording media,” IEEE Trans. Magn., 37 (2001) 1595

[15] A. G. Roy et al., “Seed-layer effect on the microstructure and magnetic properties of Co/Pd multilayers,” J. Appl. Phys. 89,

7531 (2001)

[16]N. Honda et al., “High coercivity in Co-Cr films for perpendicular recording prepared by low-temperature sputter-deposition,” IEEE Trans. Magn., 30 (1994) 4023

[17]J. K. Park et al., “Optimization of Ru intermediate layer in CoCr-based perpendicular magnetic recording media,” phys. stat. sol. (a) 201 (2004) 1763

[18]Yu-Yi Laio, “Investigation of CoPtCr-SiO2 Perpendicular Magnetic Recording Media,”the thesis research from the Advanced Storage Thin Film Lab at the National Tsing Hua University, Taiwan

[19]T. Oikawa et al., “Microstructure and Magnetic Properties of CoPtCr-SiO2 Perpendicular Media,” IEEE Trans. Magn., 38 (2002) 1976

[20]Y. Inaba et al., “Optimization of the SiO2 Content in CoPtCr-SiO2 Perpendicular Recording Media for High-Density Recording,” IEEE Trans. Magn., 40 (2004) 2486

[21]Takashi HIKOSAKA et al., “Oxygen Effect on the Microstructure and Magnetic Properties of Binary CoPt Thin Films for Perpendicular Recording,” IEEE Trans. Magn., 30 (1994) 4026

[22] Soichi Oikawa et al, “High Performance CoPtCrO Single Layered Perpendicular Media with No Recording Demagnetizatio,” IEEE Trans. Magn., 36 (2000) 2393

[23] M. Zheng et al., “Role of Oxygen Incorporation in Co-Cr-Pt-Si-O Perpendicular Magnetic Recording Media,” IEEE Trans. Magn., 40 (2004) 2498

[24] Ryoichi Mukai, Takuya Uzumaki, and Atsushi Tanaka, “Signal-to-media-noise ratio improvement of CoCrPt-SiO2 granular perpendicular media by stacked Ru underlayer,”J. Appl. Phys. 97, 10N119 (2005)

[25] Ryoichi Mukai, Takuya Uzumaki, and Atsushi Tanaka, “Microstructure Improvement of Thin Ru Underlayer for CoCrPt-SiO2 Granular Perpendicular Media,”IEEE Trans. Magn., 41 (2005) 3169

[26] J. Z. Shi, S. N. Piramanayagam, C. S. Mah, H. B. Zhao, J. M. Zhao, and Y. S. Kay, “Influence of dual-Ru intermediate layers on magnetic properties and recording performance of CoCrPt-SiO2 perpendicular recording media,”Appl. Phys. Lett. 87, 222503 (2005)

[27] S. H. Park, S. O. Kim, and T. D. Lee, “Effect of top Ru deposition pressure on magnetic and microstructural properties of CoCrPt-SiO2 media in two-step Ru layer,”J. Appl. Phys. 99,

08E701 (2006)

[28]S. N. Piramanayagam and K. Srinivasan, “Sub-6-nm grain size control in polycrystalline thin films using synthetic nucleation layer,”Appl. Phys. Lett. 91, 142508 (2007)

[29]H. Uwazumi, K. Ennomoto, Y, Sasaki, S. Takenoiri, T. Oikawa, and S. Watanabe, “CoPtCr-SiO2 granular media for high-density perpendicular recording,”IEEE Trans. Magn., 39 (2003) 1914

[30]Unoh Kwon, Robert Sinclair, E. M. T. Velu, Sudhir Malhotra, and Gerado Bertero, “Ru/Ru-Oxide Interlayers for CoCrPtO Perpendicular Recording Media,”IEEE Trans. Magn., 41 (2005) 3193

[31]S. N. Piramanayagam et al.,“Grain size reduction in CoCrPt-SiO2 perpendicular recording media with oxide-based intermediate layers,”Appl. Phys. Lett. 89, 162504 (2006)

[32]Atsushi Hashimoto et al., “Improvement of magnetic properties of granular perpendicular recording media by using a fcc nonmagnetic intermediate layer with stacking faults,”Appl. Phys. Lett. 89, 262508 (2006)

[33]S. N. Piramanayagam, H. B. Zhao, J. Z. Shi, and C. S. Mah, “Advanced perpendicular recording media structure with a magnetic intermediate layer,”Appl. Phys. Lett. 88, 092501

(2006)

[34]D. Litvinov et al., “Recording physics of perpendicular media: soft underlayers,” J. Magn. Magn. Mater. 232 (2001) 84

[35]S. Takenoiri et al., “Magnetic Properties, Magnetic Cluster Size, and Read-Write Performance of CoPtCr-SiO2 Perpendicular Recording Media ,” IEEE Trans. Magn., 39 (2003) 2279

[36]René J. M. van de Veerdonk et al., “Switching Field Distributions and ΔM Measurements for Perpendicular Media,” IEEE Trans. Magn., 38 (2002) 2450

[37]René J. M. van de Veerdonk et al., “Determination of Switching Field Distribution for Perpendicular Recording Media,” IEEE Trans. Magn., 39 (2003) 590

[38]X. W. Wu et al., “ΔM Study of Perpendicular Recording Media,” J. Appl. Phys. 93, 6760(2003)

[39]E. P. Wohlfarth, “Relations between Different Modes of Acquisition of the Remanent Magnetization of Ferromagnetic Particles,” J. Appl. Phys. 29, 595(1958)

[40]J. K. Park et al., “Optimization of Ru intermediate layer in CoCr-based perpendicular magnetic recording media,” phys. stat. sol. (a) 201 (2004) 1763

[41] T. Keitoku et al., “Preparation condition of Co-Pt-Cr-SiO2 films with high coercivity,” J. Magn. Magn. Mater. 287 (2005) 172.

[42] W. K. Shen et al., “Reduction of Ru Underlayer Thickness for CoCrPt-SiO2 Perpendicular Recording Media,” IEEE Trans. Magn. 42 (2006), 2381.

[43] T. Hikosaka, “Perpendicular Magnetic Recording medium and Magnetic Read/Write Apparatus,” US Patent No. 006,670,056 B2 (Dec. 2003)

[44] K. Sasao et al., “Concentration Dependence of the Neel Temperature ofγ-phase Mn100-xRux Alloys,” IEEE Trans Magn. 35 (1999), 3910

[45] J. K. Park et al., “Optimization of Ru intermediate layer in CoCr-based perpendicular magnetic recording media,” phys. stat. sol. (a) 201 (2004) 1763

[46] T. Keitoku et al., “Preparation condition of Co-Pt-Cr-SiO2 films with high coercivity,” J. Magn. Magn. Mater. 287 (2005) 172.

[47] W. K. Shen et al., “Reduction of Ru Underlayer Thickness for CoCrPt-SiO2 Perpendicular Recording Media,” IEEE Trans. Magn. 42 (2006), 2381.

[48] John A. Thornton, “Influence of apparatus geometry and

deposition conditions on the structure and topography of thick sputtered coatings," J. Vac. Sci. Technol., Vol. 11, No. 4 (1974), 666.

[49] T. Hikosaka, "Perpendicular Magnetic Recording medium and Magnetic Read/Write Apparatus," US Patent No. 006,670,056 B2 (Dec. 2003)

[50] K. Sasao et al., "Concentration Dependence of the Neel Temperature of γ-phase Mn100-xRux Alloys," IEEE Trans Magn. 35 (1999), 3910.